IEA EBC Annex 67

OPSYS tools for investigating energy flexibility in houses with heat pumps

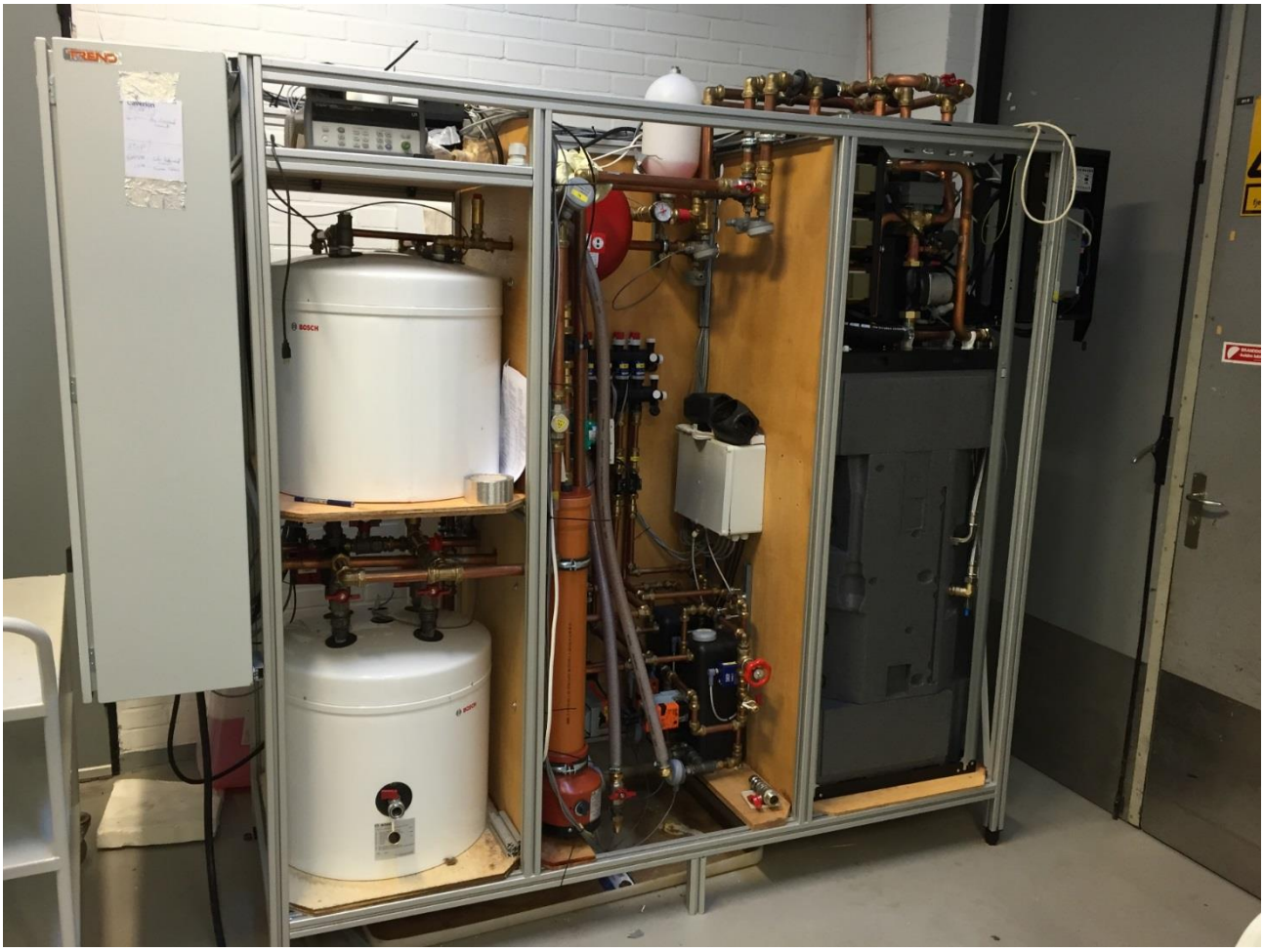

A technical report from IEA EBC Annex 67 Energy Flexible Buildings

OPSYS tools for investigation of energy flexibility in buildings

Søren Østergaard Jensen

Energy and Climate, Danish Technological Institute, Denmark

September, 2018

Preface

The increasing global energy demand, the foreseen reduction of available fossil fuels and the increasing evidence off global warming during the last decades have generated a high interest in renewable energy sources. However, renewable energy sources, such as wind and solar power, have an intrinsic variability that can seriously affect the stability of the energy system if they account for a high percentage of the total generation.

The Energy Flexibility of buildings is commonly suggested as part of the solution to alleviate some of the upcoming challenges in the future demand-respond energy systems (electrical, district heating and gas grids). Buildings can supply flexibility services in different ways, e.g. utilization of thermal mass, adjustability of HVAC system use (e.g. heating/cooling/ventilation), charging of electric vehicles, and shifting of plug-loads. However, there is currently no overview or insight into how much Energy Flexibility different building may be able to offer to the future energy systems in the sense of avoiding excess energy production, increase the stability of the energy networks, minimize congestion problems, enhance the efficiency and cost effectiveness of the future energy networks. Therefore, there is a need for increasing knowledge on and demonstration of the Energy Flexibility buildings can provide to energy networks. At the same time, there is a need for identifying critical aspects and possible solutions to manage this Energy Flexibility, while maintaining the comfort of the occupants and minimizing the use of non-renewable energy.

In this context, IEA EBC Annex 67 Energy Flexible Buildings was started in 2015 with the aim of gaining increased knowledge on the benefits and services the utilization of the Energy Flexibility in buildings may provide to the future energy networks. The present report is one among several outputs from IEA EBC Annex 67. For further information, please visit http://www.iea-ebc.org/projects/ongoing-projects/ebc-annex-67/.

Published by Energy and Climate, Danish Technological Institute, Denmark

Summary

The work of the report has been carried out in two projects financed by the Danish Energy Agency:

- Underfloor heating and heat pump optimization (abbreviated to OPSYS based on the Danish title), EUDP project no. 64014-0548
- Danish participation in IEA EBC Annex 67, EUDP project no. 64014-0573

The report presents a part of the work carried out in Danish OPSYS project (Jensen et al, 2018), the part dealing with obtaining energy flexibility via combined control of a heat pump and the heat emitting system.

Two tools were developed in OPSYS: a test rig and a fast annual simulation program. The aim of the project was to develop advanced controllers for combined control of heat pumps and heating systems in order to increase the annual performance of the systems. The two tools were also utilized for testing a simple control of the system in order to obtain energy flexibility. The resent report presents the results from these tests.

The controller decreases the set point for the room air temperatures at the start of the cooking peak (the highest peak in the Danish power grid lasting from 5pm to 8pm) and returns the set point to normal when one room starts to call for heat. It is further possible to increase the temperatures of the rooms prior to the setback in order to prolong the duration of the possible switch-off of the heat pump.

The investigations show that the controllable energy flexibility is very dependent on any free gains from solar radiation and appliances, which occur close to or during a period when energy flexibility is needed from a house. In the present investigated cases, the heat input of 3.2 kW to the main room during the one-hour cooking peak reduced the possible controllable/obtainable energy flexibility during this period. If the morning peak had been investigated, instead this would lead to more obtainable energy flexibility due to less free gains, Moreover, if the persons of the house closely after breakfast leave for job, school, etc., it would be possible to further decrease the set point temperature of the rooms.

Furthermore, the simulations show that in order to be able to offer energy flexibility to the grid during the entire heating season, the heat pump needs to be oversized. However, the additional costs of an oversized heat pumps need to be compared with the possible income from being able to offer the extra energy flexibility, which a larger heat pump makes possible.

Based on the findings from the above simulations with a very simple control strategy for obtaining energy flexibility it can be stated that in order to gain maximum energy flexibility there is a need for a more advanced controller - and preferably a controller, which includes weather forecast and forecast of free gains in the house.

Contents

List of Figures

List of Tables

1. Introduction

The increasing global energy demand, the foreseen reduction of available fossil fuels, and the increasing evidence of global warming during the last decades have generated a high interest in renewable energy sources. However, renewable energy sources such as wind and solar power have an intrinsic variability that can seriously affect the stability of the energy networks if they account for a high percentage of the total generation.

The energy flexibility of buildings is commonly suggested as part of the solution to alleviate some of the upcoming challenges in the future energy systems (electrical, district heating, and gas grids) with a large amount of fluctuating renewable energy sources. Buildings can supply flexibility services in different ways, e.g. in terms of utilization of thermal mass, adjustability of HVAC system use (e.g. heating/cooling/ventilation), charging of electric vehicles, and shifting of plug-loads.

In Denmark as well as in other western countries, heat pumps in buildings are seen as a way to obtain energy flexibility. It has been shown that heat pumps can be controlled in such a way that they can help stabilize the power grid by using less electricity during periods with large demands in the grid, while using more electricity during periods with low demands in the grid (e.g. Hedegaard, 2012, Klein et al, 2016 and Parvizi, 2016). Figure 1 shows a typical load profile of the Danish power grid. Notice the so-called cooking peak between 4 pm and 8 pm especially during the winter. There is also a smaller peak in the residential morning load. Moving the electricity demand away from these two peaks may help stabilize the power grid and make it possible to introduce more renewable energy.

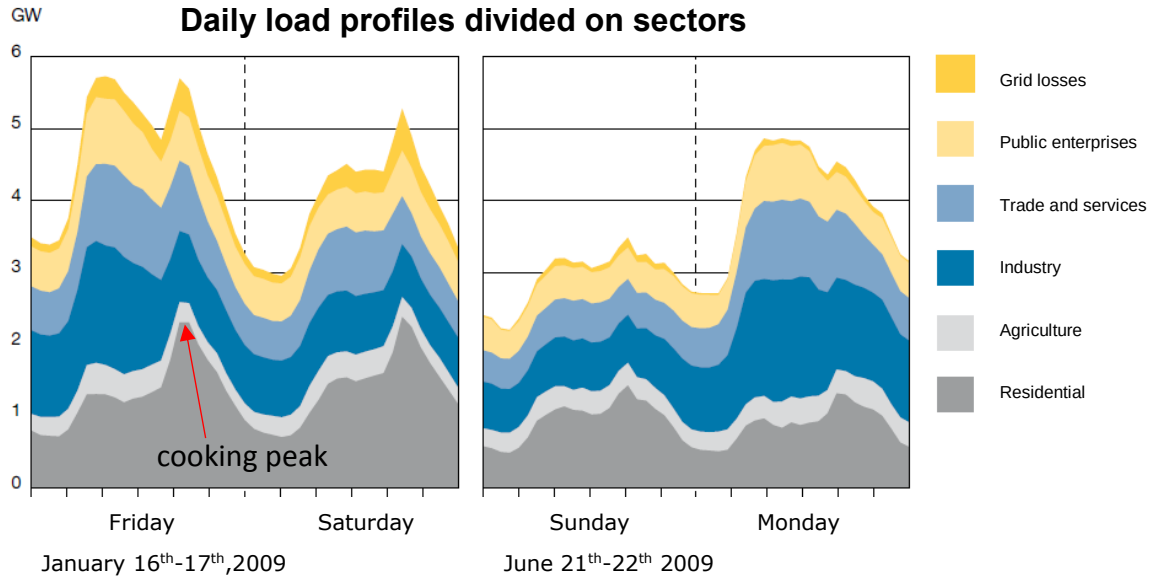

Figure 1. Typical load profiles in the Danish power grid.

Figure 2 shows an example of how the energy flexibility of houses with heat pumps can decrease the need for reinforcement of the local 0.4 kV distribution grid, where the houses are situated (Jensen et al, 2017). Figure 2 shows a winter situation for a small Danish feeder with only single-family houses.

If nothing is done and if heat pumps are introduced in all houses and 40 % of the houses has an electrical vehicle (EV), the maximum allowed load will be excessed during the cooking peak in the wintertime. However, if the houses are excess heated prior to the cooking peak while maintaining the room temperature within the comfort range, most of the heat pumps may be switched off during the cooking peak. In order to stay below the maximum allowed load, the VEs should, furthermore, be charged intelligently and not at full speed during the

cooking peak. After the cooking peak there will be a rebound effect, where the heat pumps may need more electricity to increase the room temperature from the lower temperature of the comfort band.

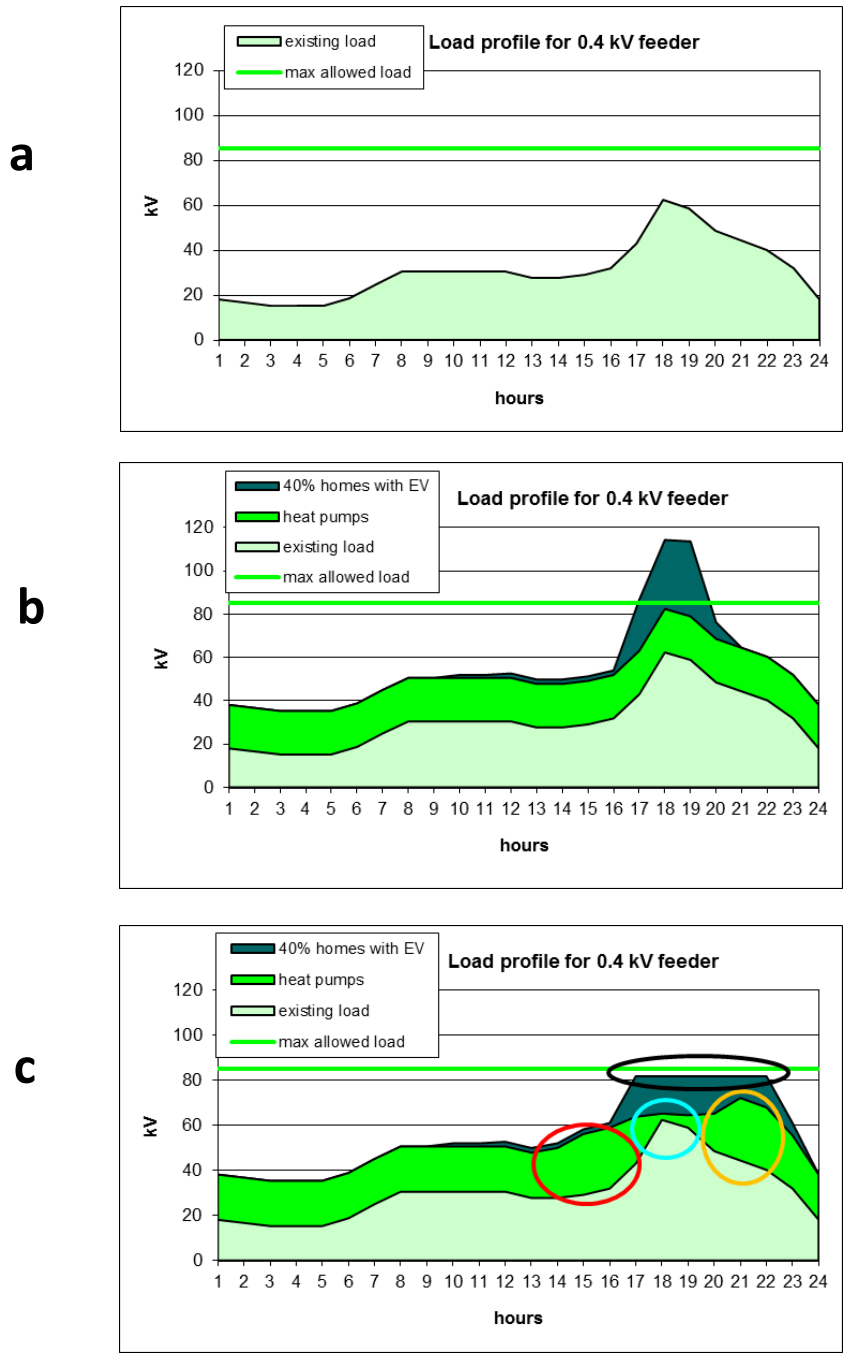

Figure 2. An example of the introduction of heat pumps and electrical vehicles in a 0.4 kV outlet/feeder (Jensen et al, 2017):

a) the existing situation. The peak from 5pm to 8pm is called the cooking peak due to people coming home from work and start cooking. The peak is also due to the switching on of other appliances.

b) business as usual: heat pumps and electrical vehicles (EVs) in the system will demand a reinforcement of the grid as the demand exceeds the maximum allowed load

c) a Smart Grid solution where the buildings prior to the cooking peak (5pm-8pm) are excess heated within the comfort band of the room temperature (red circle). The buildings are mainly free floating during the cooking peak (blue circle), but they need extra heat after the cooking peak (orange circle). The charging of the EVs is controlled intelligently in order to keep the demand below the maximum allowed load (black circle).

The utilization of heat pumps to obtain energy flexibility has been investigated in several projects, both Danish and international projects – e.g. iPower (www.ipower-net.dk), EcoGrid 1.0 and 2.0 (http://www.ecogrid.dk/en/homeuk) and IEA EBC Annex 67 Energy Flexible Buildings (www.annex67.org).

The German smart grid ready label (www.waermepumpe.de/sg-ready/) deals with the control of heat pumps in order to obtain energy flexibility. This has also been the case in several Danish projects dealing with demand response through the control of heat pumps. However, it is often not possible to obtain the full energy flexibility of a house, when only controlling the heat pump (Jensen et al, 2016). It is not possible to excess heat the building before switching off the heat pump, which otherwise would have made it possible to further prolong the switch off period. In order to excess heat a house, one has to be able to control the thermostats of the heat emitters as well, - i.e. one has to be able to increase the set point of the thermostats for a period in order to be able to deliver energy to the house and increase the room temperature above the normal set point of the thermostats, while still being inside the comfort range.

Combined control of heat pumps and the heat emitting system was carried out in the OPSYS project (Jensen et al, 2018).

1.1 The OPSYS project

The purpose of the OPSYS project was to minimize the gap between the accredited efficiency of a domestic heat pump and the actual efficiency when installed in a house. Unfortunately, measurements on existing heat pump installations have shown Seasonal Performance Factors (SPF: mean annual COP (efficiency)) well below expectations as the heat pump and the heat emitting system are rarely properly adjusted at the installation of the heat pump (Poulsen et al, 2017). For example, the forward temperature (often also called supply temperature) from the heat pump is often set too high in order to guarantee sufficient space heating. A forward temperature higher than needed results in a lower COP.

Typically, an increase of 1°C of the forward temperature leads to a decrease of 2-3% of the COP. For most heat pumps, the only control and means of reducing the forward temperature is a simple ambient temperature correction, which, however, rarely leads to an optimal forward temperature. When the forward temperature is too high, it also has consequences for the heat emitting system. The volume flow through the system fluctuates due to uncoordinated opening and closing of the valves in the system, e.g. manifold valves for an underfloor heating system. The higher the forward temperature is above the minimum required forward temperature, the more the amplitude of the fluctuations increases. The fluctuating flow causes the heat pump to fluctuate in produced heating power resulting in a reduced COP compared to the optimal COP at the actual temperature level. The larger fluctuations, the higher decrease in efficiency (Jensen, Olesen and Paulsen, 2014).

A too low pressure drop across one of the heat emitters will lead to a too high flow rate through this heat emitter. This will leave less flow rate for the other heat emitters, which then will require a higher forward temperature in order to be able to satisfy the heat demand of the rooms with a too low flow rate. A high forward temperature leads to a poorer COP for the heat pump.

A recent study on the performance of more than 160 Danish heat pumps (Poulsen et al, 2017) reveals that only around 15 % of the heat pumps perform as expected. The main reasons are, besides installation errors and too small heat emitters, that the flow rate through the differing heat emitters is wrongly adjusted and that the heating curve of the heat pump is set too high leading to potential combined savings of up to 25 %.

The aim of the OPSYS project was to minimize these problems, so that end users receive the expected efficiency from their heat pump installations. The goal was, therefore, to develop integrated controllers for the heat pumps and the heat emitting systems to reduce the forward

temperature and the fluctuations of the flow rate in the system. An optimized controller, which controls both the forward temperature from the heat pump and the valves of the heat emitting system will, therefore, lead to a more efficient heat pump installation.

1.1.1 The OPSYS tools

The aim of the project was to develop new and more advanced control strategies in order to increase the efficiency of heat pump installations. For the purpose of facilitating this, two tools have been developed during the OPSYS project: a test rig and a fast, annual simulation program. The rationale for this was:

1. demonstration in real houses is preferable, however, there are many non-controllable variables in a real house, which makes it difficult to draw reliable, significant conclusions - unless the control is demonstrated in several houses. Moreover, the demonstration in real houses is time consuming and very expensive
2. simulation is cheap and fast, but it lacks somewhat credibility since all inputs and the environment are fully specified and often in a very simple way, which may lead to conclusions that are not likely in real life
3. hardware in the loop (e.g. the OPSYS test rig) establishes a bridge between the two approaches described above. In the OPSYS test rig, some inputs are controllable, while the environment is realistic, but, different from real houses, repeatable

As combined control of both the heat pump and the heat emitting system is a new field, 1) demonstration in real houses was not within the scope of the project. However, it is believed that based on the obtained results from the OPSYS project, a follow-up project may include tests in real houses.

Tool 2) and 3) are both needed because tests in the test rig are conducted in real time – i.e. it takes a year to test a year. Therefore, only shorter and very precise tests should be carried out in the test rig. However, in order to facilitate the development of the combined controllers, there is a need for a very fast tool (i.e. tool 2)) for obtaining quick results and for performing various parametric analysis. In order to make tool 2) very fast, it is necessary to introduce several simplifications about the heat pump and heat emitting system. However, to gain confidence in the concept before moving the control strategies to real houses, there is a need for testing the concepts in a "hardware in the loop" system with a real heat pump and a semi-real heat emitting system – i.e. tool 3).

The two tools are briefly described in the following chapter.

1.1.2 Simple test for obtaining energy flexibility

The present report describes the results from tests of the OPSYS tools for obtaining energy flexibility. A very simple controller was chosen for the tests. The controller decreases the set point for the room air temperatures at the start of the cooking peak and returns the set point to normal when one room starts to call for heat. It is further possible to increase the temperatures of the rooms prior to the setback in order to prolong the duration of the possible switch-off of the heat pump.

2. OPSYS test rig and simulation tool

A dynamic experimental setup has been constructed – further information may be found in (Jensen et al, 2018). The system (test rig) emulates a house with an underfloor heating system to which a ground source heat pump can be connected. Figure 3 shows a principle sketch of the system. The system has two main elements denominated the hot side and the cold side, seen from the heat pumps point of view (cold side = evaporator side, hot side = condenser side).

The hot side emulates the underfloor heating system with the possibility of using a buffer tank. The underfloor heating system is emulated via a series of parallel-connected heat exchanges resembling each room in a house. In order to reduce the complexity of the test rig, the house is emulated by only four zones. The number of zones of the house may later be extended on the test rig. Hot water draw off may also be emulated, but this is currently not part of the test setup.

The control of the experimental setup is a simulation program that controls the heat consumption (via an embedded FMU of the considered house) and provides the BMS controller of the test rig with a return temperature and a valve position for each "room". In this way, it is, on one hand, possible to control an underfloor heating system like in an ordinary house, while it, on the other hand, makes it possible to test different, advanced control strategies. The size and function of the "rooms" can easily be changed by changing the load patterns and temperatures of the "rooms" in the simulation program.

The simulation program also controls the forward temperature of the heat pump. In the present set up, the physical ambient temperature sensor is replaced by a signal from the simulation program and utilizes the heating curve of the heat pump.

The cold side of the experimental setup (see figure 3) emulates a heat source, e.g. the ground. This is an electric heater, which is controlled by the simulation program in order to emulate the temperature of the brine to the cold side of the heat pump. With this method seasonal variations in the brine temperature and different lengths of tubes in the earth can be emulated.

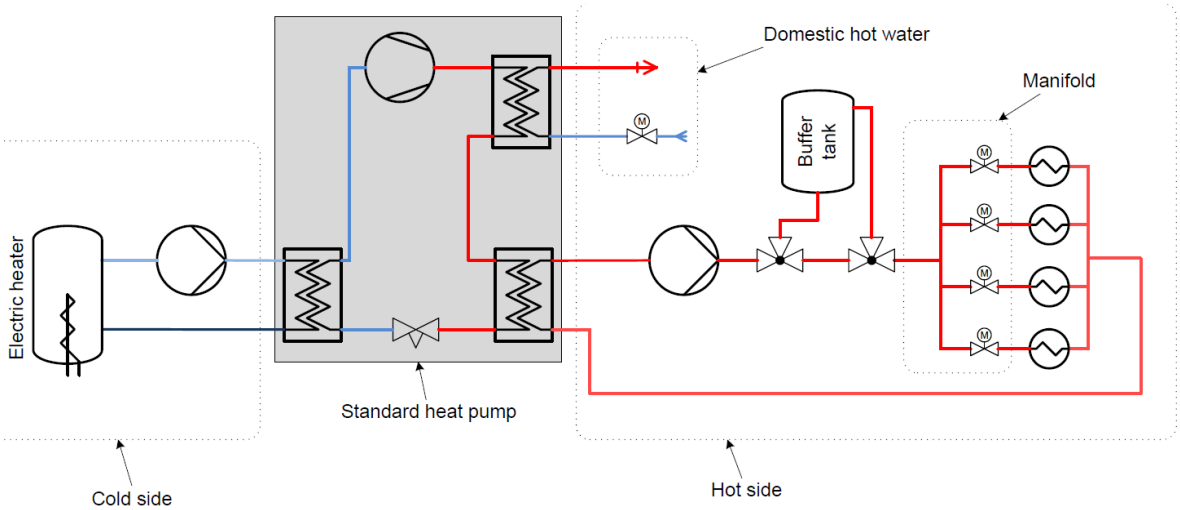

Figure 3. Principle sketch of experimental setup.

The simulation model running on the pc of the test rig is a phyton (programming language) script, which controls the BMS (Building Management System from Trend) on the test rig and an external data logger. In order to facilitate the use of a Dymola FMU (Functional

Mock-up Unit) in the python scripts, a special pyFMI script was developed to facilitate communication via Modbus between the BMS at the test rig and the simulation pc.

The Trend GUI running on the simulation pc for setting up a test, viewing the progress of a test and logging measured data from the BMS is called 963. The main screens of the 963 are shown in figures 4-6. Figure 4 shows the screen for viewing the four underfloor heating circuits. The main purpose of this part of the test rig is to emulate the heating system of the house, including securing the return temperature from the four heat exchanges as specified by the simulation program. Figure 5 shows the brine side of the test rig, while figure 6 shows the connection between the test rig and the central cooling system of the laboratory, where the OPSYS test rig is situated. The cooling system shown in figure 6 is responsible for providing the heat demand of the house, which the simulation specifies. For more information on the OPSYS test rig, please see (Jensen et al, 2018, Appendix A).

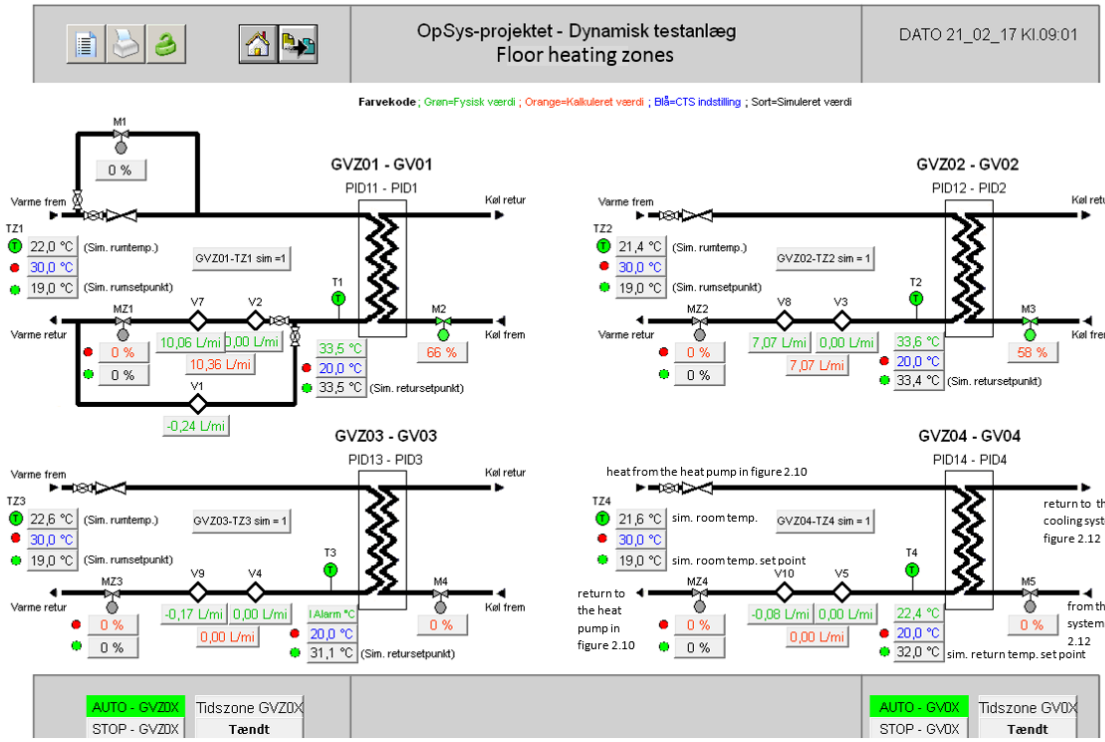

Figure 4. The BMS screen for viewing and controlling the four heating zones of the test rig.

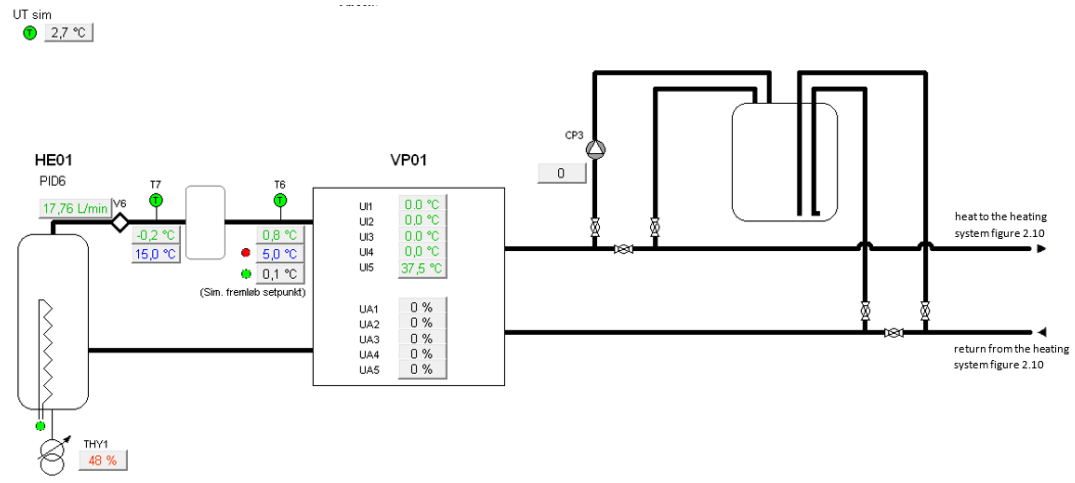

Figure 5. The BMS screen for viewing and controlling the heat pump and the brine side of the test rig.

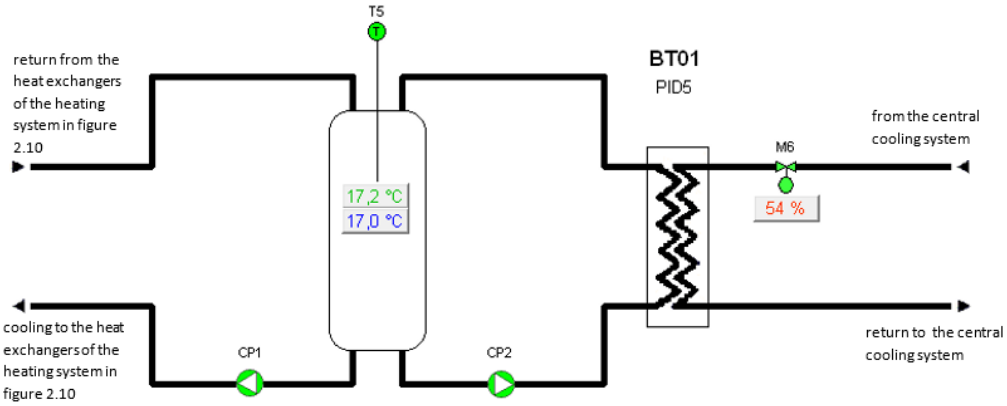

Figure 6. The BMS screen for viewing the controlling of the cooling system of the test rig.

In the simulation program running on the test rig pc, it is possible to introduce and investigate different control strategies of the forward temperature from the heat pump and the position of the valves of the four heat exchangers emulating the heat emitters of the house. The control strategies developed by using the annual simulation program may, therefore, directly be implemented in the control of the test rig.

2.1 The annual simulation program

The core of the annual simulation program is a model of a typical Danish house. The same model is used in the simulation program running on the test rig pc. The house model is developed in Dymola (Modelica) and imbedded in a python script as a FMU (Functional Mock-up Unit). The house model includes all constructions of the house (walls, windows, ceiling, etc.), the underfloor heating system of the four rooms, internal gains (people and appliances), external gains (solar radiation through windows), and the ambient temperature.

Figure 7 shows a top layer view of the house model with constructions, while figure 8 shows the elements of the heating system including the four underfloor heating circuits in details.

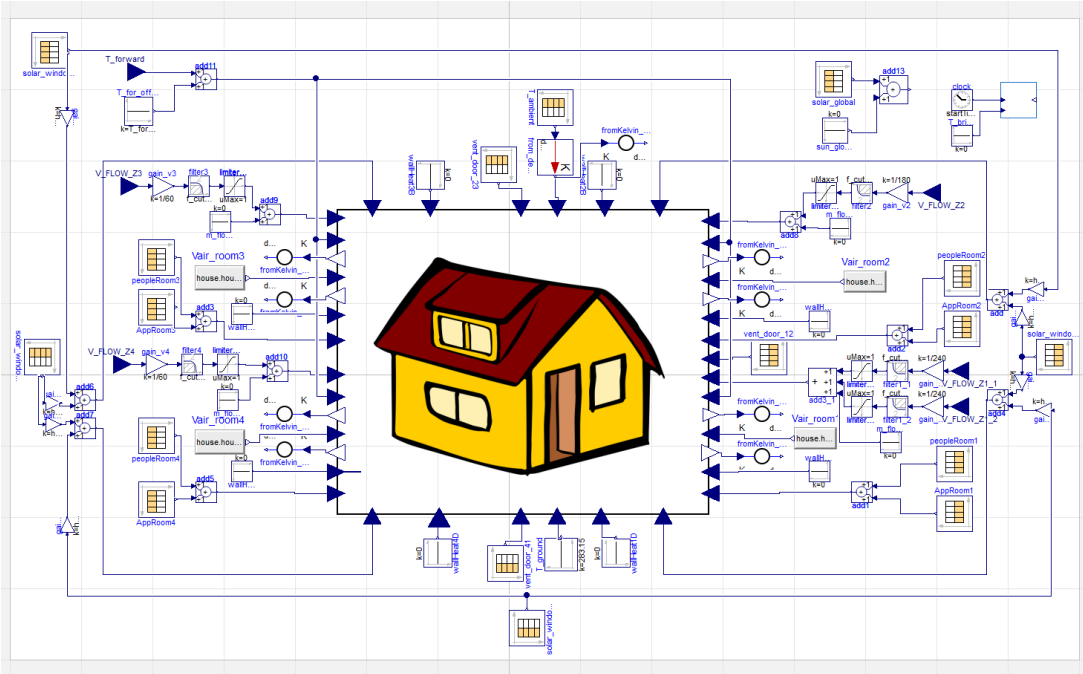

Figure 7. Top layer view of house simulation model.

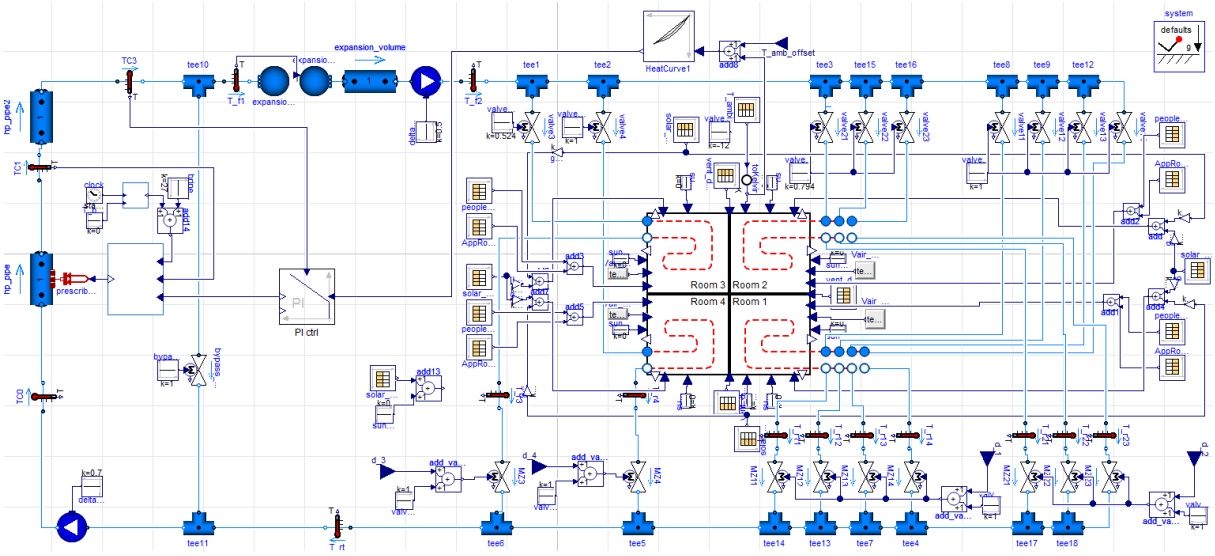

Figure 8. Overview of the heating system in the house model.

The main differences between the simulation program on the test rig and the annual simulation program are:

- the simulation program on the test rig runs in real time. The annual simulation program is much faster.
- the simulation program on the test rig controls a real heat pump, while the heat pump in the annual simulation program is virtual

Originally, the idea of the virtual heat pump in the annual simulation program was to utilize the detailed heat pump model from Dymola. However, the computation time of this was too long to facilitate a fast, annual simulation. A simpler model was, therefore, chosen for the annual simulation program. However, work has, as part of OPSYS, been carried out to accelerate the speed of the heat pump model in Dymola.

A very simple representation of the heat pump was taken from another project (Jensen, Christensen, Jørgensen and Huet, 2016) based on a regression of test results for a specific heat pump not identical to the heat pump in the test rig:

$$\Delta T = (T_h - T_c) \quad [1]$$

$$COP_{carnot} = T_h / \Delta T \quad [2]$$

$$COP_{HP} = eta * COP_{carnot} \quad [3]$$

$$eta = -0.02623*P + 0.0010993*\Delta T + 0.4016 \quad [4]$$

$$Q_H = P * COP_{HP} \quad [5]$$

where: COP_{carnot} is the system Carnot COP based on the forward temperature from the heat pump and the brine temperature to the heat pump

T_h: is the forward temperature from the heat pump [K]

T_c: is the brine inlet temperature to the heat pump [K]

COP_{HP}: is the "real" COP of the heat pump at the actual operating conditions

eta: is the system Carnot efficiency of the heat pump

P: is the electrical power to the heat pump [kW]

Q_H: is the calculated heat produced by the heat pump [kW]

For further information on the simple heat pump representation, please see (Jensen, Christensen, Jørgensen and Huet, 2016).

The performance of the simple representation of the heat pump in the annual simulation program is dealt with in chapter 5.

The python script of the simulation program on the test rig and the annual simulation program include control options for controlling the performance of the heat pump and the heat emitting system. Two control options have been tested in the test rig: a typical uncoordinated on/off control of the valves (telestats) of an underfloor heating system and an on/off control for obtaining energy flexibility from a house with a heat pump (see chapter 4). Furthermore, it is possible to implement highly advanced controls in both simulation environments.

3. Simple set point modulation

The standard for indoor climate EN 15251 states that the indoor temperature preferred by most people is 22°C±2 K during the heating season for mainly sedentary work and with typical clothing. However, more sensitive people would prefer a more narrow comfort band like 22°C±1K.

The above comfort bands allows both for excess heating and switching off the heat pump during certain periods dependent on the use and heat demand of the house. In the following, this is utilized to shift the electricity demand of a heat pump away from the cooking peak in the afternoon/evening.

Figure 9 shows a situation where the set point of the room temperature is lowered at the start of the cooking period – here starting at 5pm. The blue line in figure 9 is the normal control of the house, where the room temperature is kept at 22°C during the day, while set to 19°C during the period 11pm to 6am - night setback. This is quite normal in Danish houses. The set point modulation for obtaining flexibility is shown with a red line in figure 9. At the start of the cooking peak the set point is decreased – here 1 K. The duration of this set back is determined by the room temperature in the rooms. When the temperature in one room gets below the setback temperature – 21°C in figure 9, the heat pump is restarted, and the heating system will bring the room temperatures back up to normal – here 22°C. The duration of the setback is given by the allowed fluctuation of the room temperatures, the heat demand of the house (taking into account heat gains from persons, appliances, and solar radiation), and the amount of heat stored in the walls, ceiling and floor. Thus, the possible duration of the setback is longer at high ambient temperatures and in houses with a large internal thermal mass.

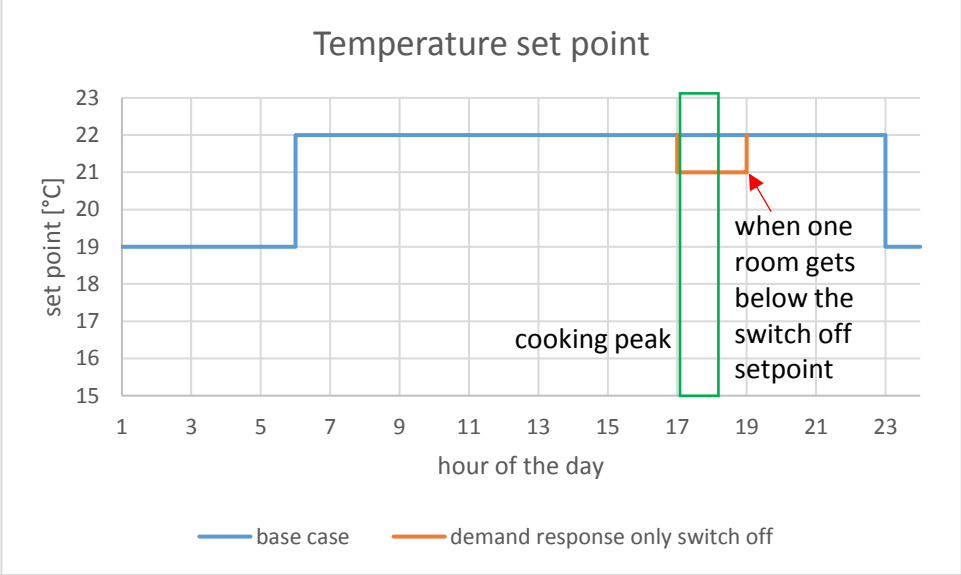

Figure 9. Test focussing on only switching off the heat pump.

If the duration of the setback is short and ends before it is time for the night setback, there is a rebound effect, which means that the heating system often needs to emit more heat than saved during the setback in order to return the room temperatures to the normal set point temperatures (blue line in figure 9). If, however, the duration of the setback is longer and continues until the time of the night setback, there will be no rebound effect, and energy may actually be saved compared to normal operation. The duration of the setback may be increased if the temperature of the rooms prior to the setback is increased, but still being within the range of comfort. Figure 10 shows this situation.

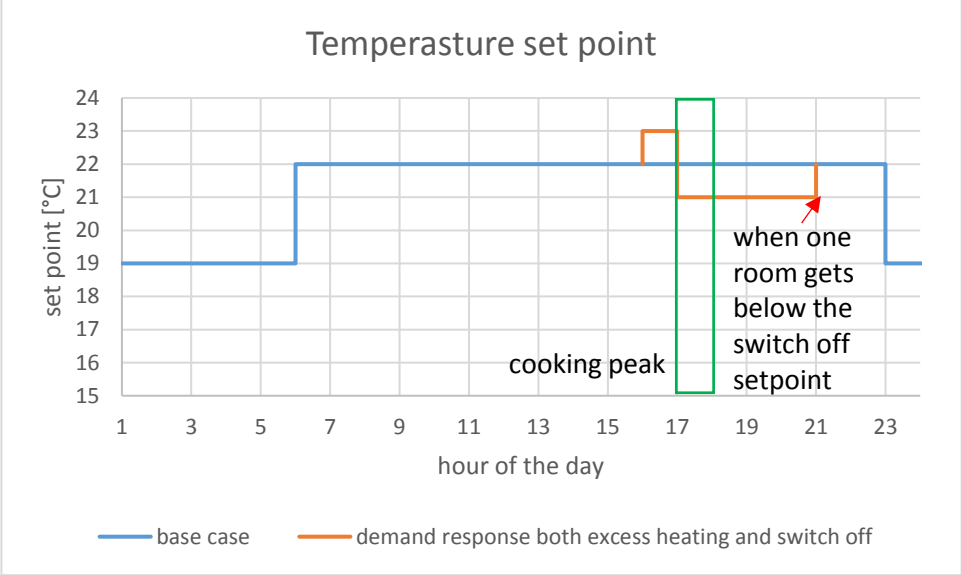

Figure 10. Test with both switching off the heat pump and excess heating.

Both situations in figures 9 and 10 will be investigated in the following chapter. Figure 11 shows the different parameters of interest in the investigation.

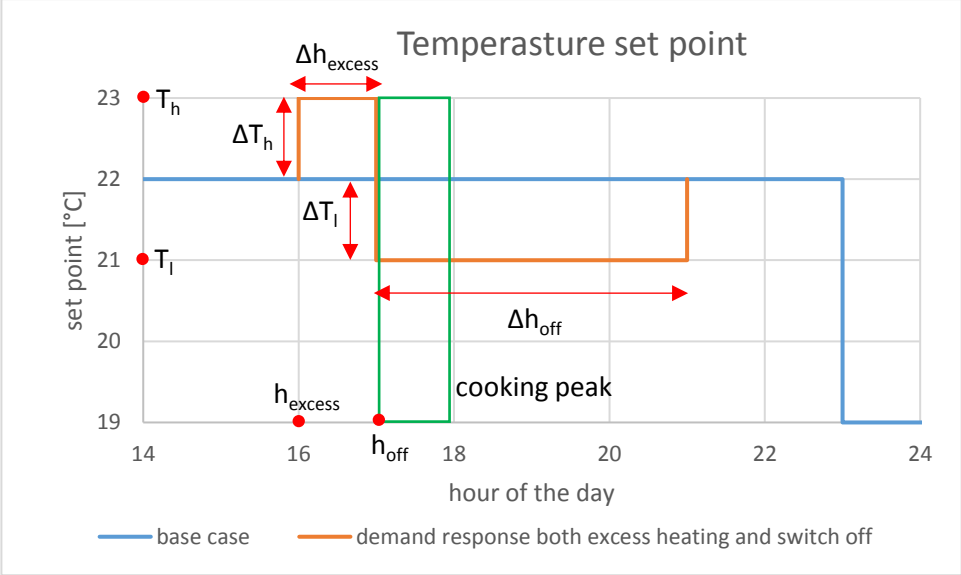

Figure 11. Parameters of interest in the investigation:
T_h: room temperature set point for excess heating
T_l: room temperature set point for setback during the switch off period
ΔT_h: aimed temperature increase during excess heat
ΔT_l: maximum allowed temperature decrease during switch off
h_{excess}: time for start of excess heating
h_{off}: time for switching off the heating
Δh_{excess}: duration of excess heating
Δh_{off}: duration of switching off heating

The duration of the switch off Δh_{off} depends on:

- T_h: room temperature set point for excess heating
- T_l: the setback room temperature set point
- Δh_{excess}: duration of excess heating

A parametric study, where these three parameters are varied, are, therefore, carried out. The following tests are performed, where the baseline test is the situation with no modulation of the temperature set point – i.e. the blue line in figures 9-11.

3.1 Baseline test

The baseline is with traditional on/off control of the valves of the underfloor heating system. The result from this test is the basis to which the other tests primarily are compared.

3.2 Only switching off the heat pump

The following is superimposed the baseline test – see also figure 9:

- at 5pm (h_{off}), when the cooking peak starts, the set points of the room temperature in all rooms are decreased with ΔT_l to T_l
- the set point temperature remains T_l until the temperature in <u>one</u> room gets below T_l. At this point the set point of all rooms is changed back to the original set point at 22°C (the set point is always reduced to 19°C during the night) and the heat pump is started

3.3 Both switching off the heat pump and excess heating

The following is superimposed the baseline test – see also figure 10:

- at h_{excess}, the set point of the room temperature in all rooms is increased by ΔT_h to T_h
- at 5pm (h_{off}), when the cooking peak starts, the set points of the room temperature in all rooms are decreased with $\Delta T_h + \Delta T_l$ to T_l
- the set point temperature remains T_l until the temperature in <u>one</u> room gets below T_l. At this point the set point of all rooms is changed back to the original set point at 22°C (the set point is always reduced to 19°C during the night) and the heat pump is started

3.4 Parameter variation

The following parameter variations seems interesting:

- T_h: 23°C and 24°C
- T_l: 21°C and 20°C
- h_{excess}: 3pm and 4pm

4. Simulated set point modulation

The parametric study described in the former chapter has been carried out using the annual simulation tool as the test rig runs at real-time and, therefore, not allowing for annual parameter studies. The chosen house is a Danish single-family house from the 70's. The house has a floor area of 150 m². The house model is identical to the one used in the OPSYS test rig. As the test rig currently only has four physical circuits emulating the underfloor heating system, the house model is also simplified to a four-room model as seen in figure 12.

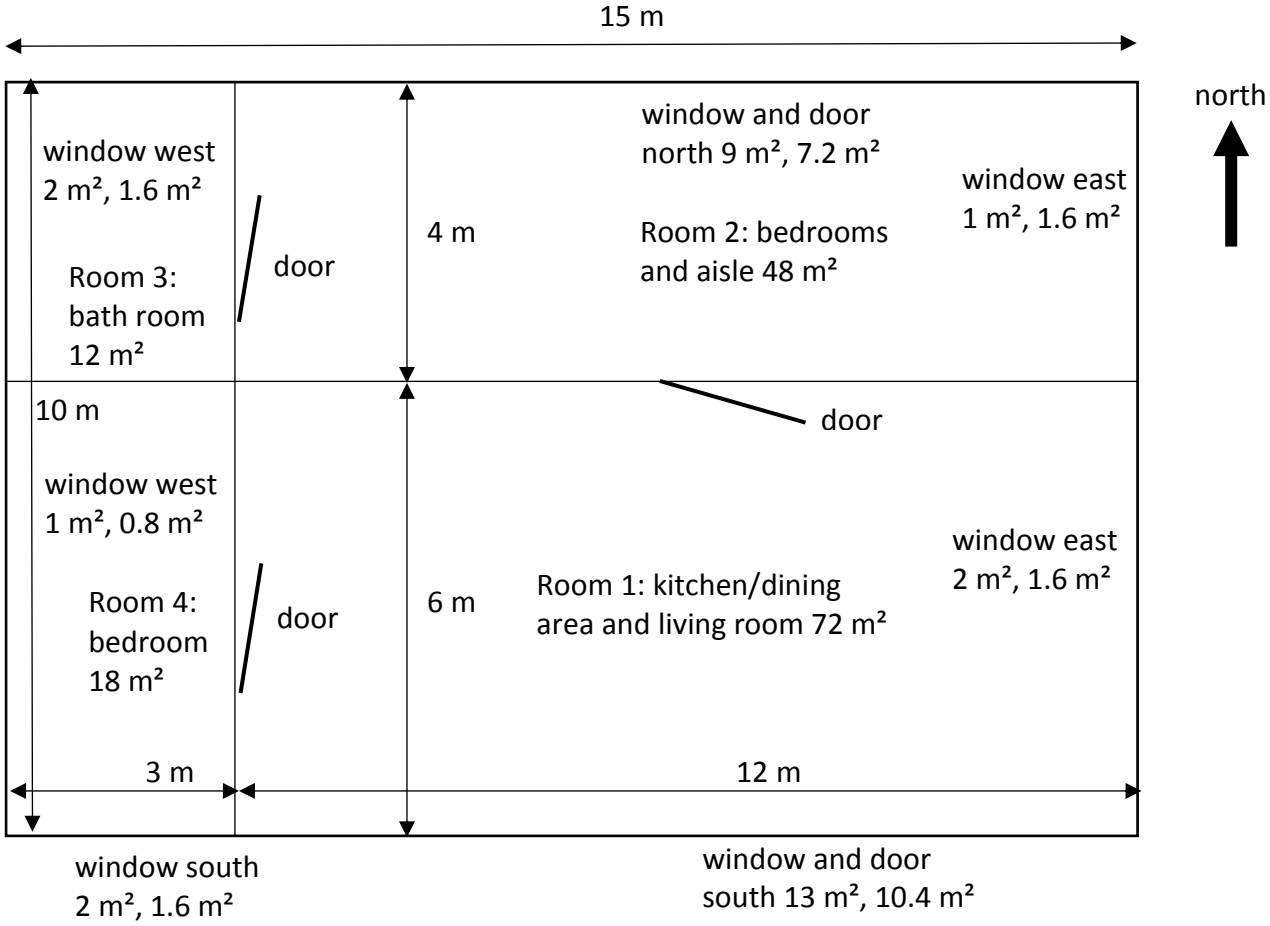

Figure 12. Floor plan of the building model. The two numbers for the windows and doors are: the first number is the total area incl. framing, and the second number is the transparent area.

The underfloor heating in the three rooms 1, 2 and 4 is lightweight, while it is heavy in room 3 (the bathroom). Thus, the heating up after switching on the heat pump is slower in room 3 than in the other three rooms.

The internal gains from appliances and persons are described in details in (Jensen et al, 2018 - Appendix C). Weather conditions, solar radiation to the rooms, and temperature of the brine to the heat pump are also described in (Jensen et al, 2018 - Appendix C).

The heat pump installed in the house is a ground coupled heat pump with an SPF (Seasonal Performance Factor = annual efficiency) of around 3.5. In this study, the heat pump only delivers space heating in order not to complicate things, as the domestic hot water (DHW) demand is very stochastic. Excess heating of a DHW tank may, however, add extra energy flexibility to a house, but it is not within the scope of this document.

The heat pump is frequency controlled in the range of 0.5-2.5 kW electricity and on/off controlled below 0.5 kW electricity.

The below U-value for the constructions are typical for Danish houses from the 70'es. The below values for the capacity are for the fabric exposed to indoor, which for the external constructions is the fabric between the indoor air and the insulation in the construction and for the window the inner glass.

		U-value	Capacity
external walls:	bricks + insulation:	0.60 W/m²K	118,800 J/m²K
floor rooms:	wooden floor + insulation	0.18 W/m²K	21,560 J/m²K
floor bathroom:	concrete + insulation	0.18 W/m²K	180,000 J/m²K
ceiling:	wood + insolation:	0.20 W/m²K	16,900 J/m²K
internal walls:	lightweight concrete	1.41 W/m²K	68,000 J/m²K
windows:	2 layered traditional glazing:	2.80 W/m²K	8,100 J/m²K
ventilation:	natural: 0,3 l/s/m²		

Heat is not only exchanged between rooms via conduction through walls. Larger heat exchanges occurs often via air movements through doors between rooms. The inter-zonal airflow through doors V_d (mixing flow) is approximated using an empirical relationship (Design Builder Software Ltd, 2016) calculated as:

$$V_d = A_d \alpha_d V_f$$

where: A_d is the door area – here 2 m²,
α_d is the door opening in %,
V_f is the Farea-flow (set to 0.1 m³/m²/s).

Furthermore, a schedule is used to set how the door between room 1 and 2 (see figure 12) is open based on occupancy information (50% open from 7 to 21 on weekdays, 50% open from 9 to 21 in the weekend, and 0.25% open in-between due to leakage beneath the door). The two other doors between room 2 and 3 and room 1 and 4 are mostly closed and a fixed opening of 1.25% is used all the time (averaged occasional opening and leakage).

4.1 Baseline simulation

The baseline simulation is performed with a traditional on/off control of the valves to the four underfloor circuits. The thermostats have a hysteresis of ±0.5 K.

The annual space heating demand has been calculated to 16,904 kWh, while the annual electricity demand of the heat pump was 4,877 kWh. This gives a SPF of 3.47, which constitutes a good heat pump installation (Poulsen et al, 2017). The monthly sums of electricity to the heat pump are shown in figure 13.

As the setback of the room temperature for energy flexibility purposes starts at 5pm and ends at 11pm, when the night setback is activated, the maximum amount of shiftable energy is the electricity demand of the heat pump during the six hours between 5pm and 11pm. This potential is often not available as the room temperature during cold periods drops below the setback temperature before the time of the night setback is reached. This will be investigated in the following. However, first the potential amount of shiftable energy will be investigated.

Figure 14 shows the daily amount of shiftable electricity over the year. The maximum amount of shiftable energy is of course highest during the winter where the largest heat demand occurs. Figure 15 shows the same values as figure 14, but now as a function of the daily mean ambient temperature for the respective daily amount of shiftable electricity demands.

Figure 15 shows a fair correlation between the maximum daily amount of shiftable electricity demands and the corresponding mean daily ambient temperatures. The scattering of the values is due to the solar radiation entering the rooms. A high daily amount of solar radiation leads to a lower maximum amount of shiftable electricity demand.

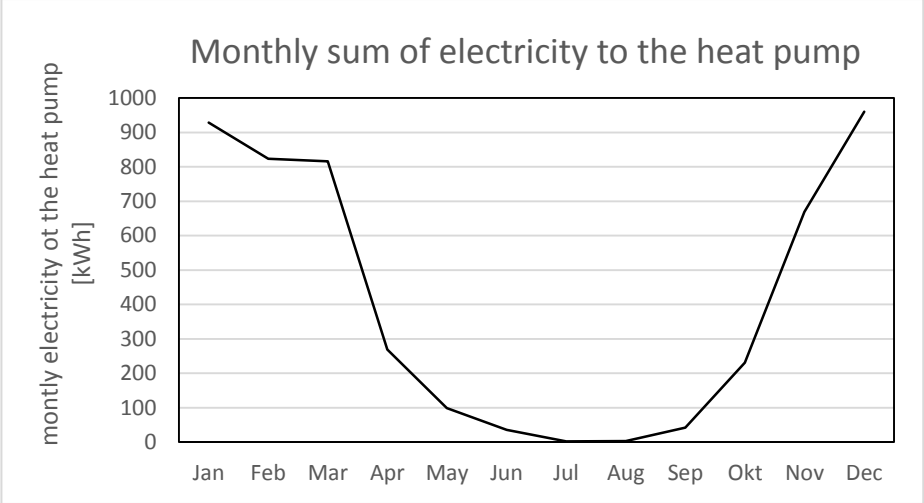

Figure 13. Monthly sums of the electricity demand of the heat pump in the baseline simulation.

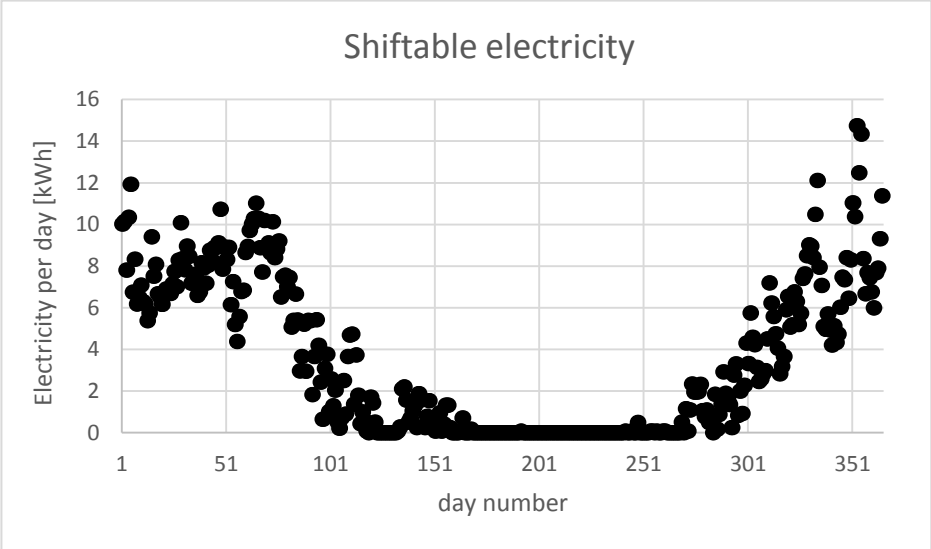

Figure 14. The maximum daily amount of shiftable electricity during the period 5pm-11pm.

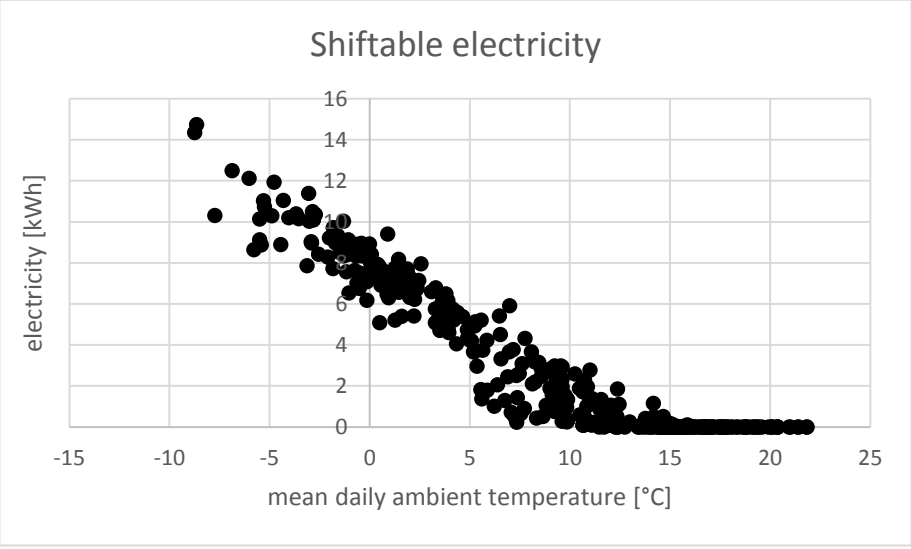

Figure 15. The maximum daily amount of shiftable electricity from figure 15 dependent on the daily mean ambient temperature.

4.2 Parametric study

The three parameters:

- T_h: room temperature set point for excess heating
- T_l: the setback room temperature set point
- Δh_{excess}: duration of excess heating

May be varied in different ways. The following could be interesting:

0U0H1D: T_l = 21°C, no excess heating
0U0H2D: T_l = 20°C, no excess heating
1U1H1D: T_l = 21°C, T_h = 23°C starting at 4pm
1U2H1D: T_l = 21°C, T_h = 23°C starting at 3pm
1U1H2D. T_l = 20°C, T_h = 23°C starting at 4pm
1U2H2D: T_l = 20°C, T_h = 23°C starting at 3pm
2U1H1D: T_l = 21°C, T_h = 24°C starting at 4pm
2U2H1D: T_l = 21°C, T_h = 24°C starting at 3pm
2U1H2D: T_l = 20°C, T_h = 24°C starting at 4pm
2U2H2D: T_l = 20°C, T_h = 24°C starting at 3pm

Where: T_l: setback temperature (D for down = setback of temperature)
T_h: excess heating temperature (U for up = increase of room temperature)
H: number of hours for the start of excess heating before the start of the cooking peak)

4.3 Detailed results from parameter variation 1U1H1D

Before presenting the results of all parameter variations one variation will be described in more details to explain different aspects of the effect of excess heating and forced switching-off of the heat pump. The selected variation is 1U1H1D, whichs means that the set point of the rooms temperatures is increased to 23°C (1U) one hour before the cooking peak (1H), while the set points are decreased to 21°C at the start of the cooking peak (1D) – i.e. the situation shown in figure 10.

The following results are from investigations with the chosen house, climate conditions, use, control strategy, etc. Thus the obtained conclusion may not be true for other houses in other countries with different use or control. The purpose is to investigate the influence of excess heating and temperature setback on the room temperatures, duration of setback, and the possible shift of energy.

The overall result of the 1U1H1D control strategy is an annual space heating demand of 16,877 kWh and an annual electricity demand of 4,876 kWh at a SPF of 3.46. The heat and electricity demands are similar, but they are surprisingly slightly lower than for the baseline case. A somewhat higher electricity demand was expected due to the higher heat loss during the one hour of excess heating. The reason for this is that the rebound effect expected after the forced switching-off of the heat pump often does not or hardly occurs because of the night setback. This is shown in the following.

Figure 16 shows the development of the room temperatures during January 4. Figure 16 shows that the heat pump has difficulties bringing the room temperatures up again after the night setback due to a cold day (between -5 and 0°C) and little solar radiation. Especially room 4 suffers from a low room temperature due to the large external surface to floor ration. The cooking peak in the house is clearly seen at the curve for the kitchen/living room (room 1). The influence of the heavy floor heating in the bathroom (room 3) is also clearly seen: the room only cools down slowly during the night, while the excess heating (5pm-6pm) hardly is seen. The setback of the temperature to 21°C lasts only for 1 hour and 20 minutes due to the cold weather conditions. The temperature of the north facing room 2 is mostly influenced by

the setback, and it is the temperature, which activates the restart of the heat pump. Due to the slow underfloor heating system, the hysteresis of the heat emitting system is more than ±0.5 K (as defined in the simulation model) – it is rather ±0.7 K.

Figure 17 shows the power to the heat pump and the heat demand of the house during January 4th for the baseline case, and figure 18 shows this case for the 1U1H1D simulation.

Figure 17 shows a dip in the consumed power and the produced heat of the heat pump at approximately 1pm. The dip is caused by the thermostat of the kitchen/living room being switched off as the room temperature in this room reaches 22.5°C as seen in figure 16. A closer look at the energy demand to the four rooms reveals that room 1 is responsible for nearly half of the heat demand of the house on January 4th. On an annual basis, 42 % of the heat produced by the heat pump is delivered to room 1, 34 % is delivered to room 2, and 12 % is delivered to each of room 3 and 4.

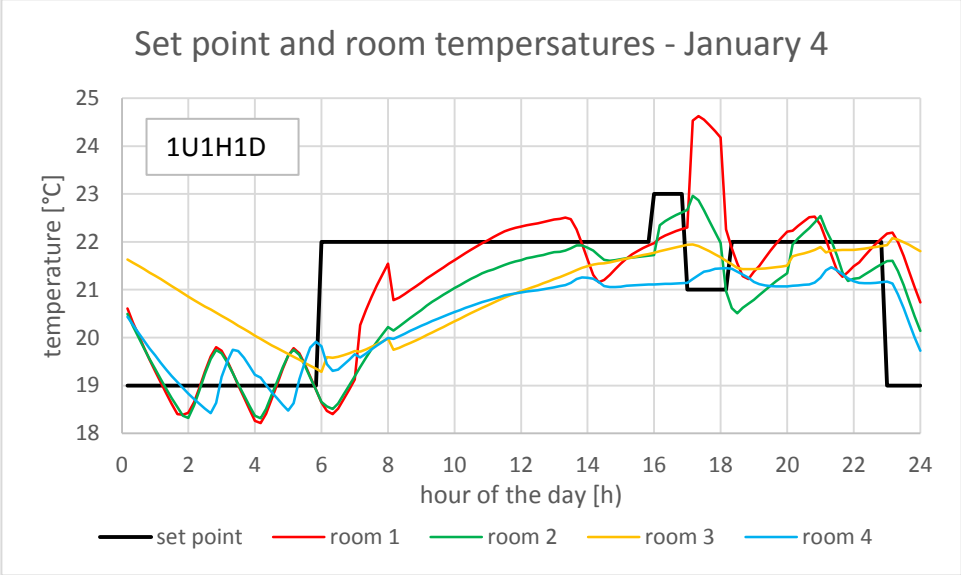

Figure 16. The evolution of the set point and room temperatures during January 4th for the simulation 1U1H1D.

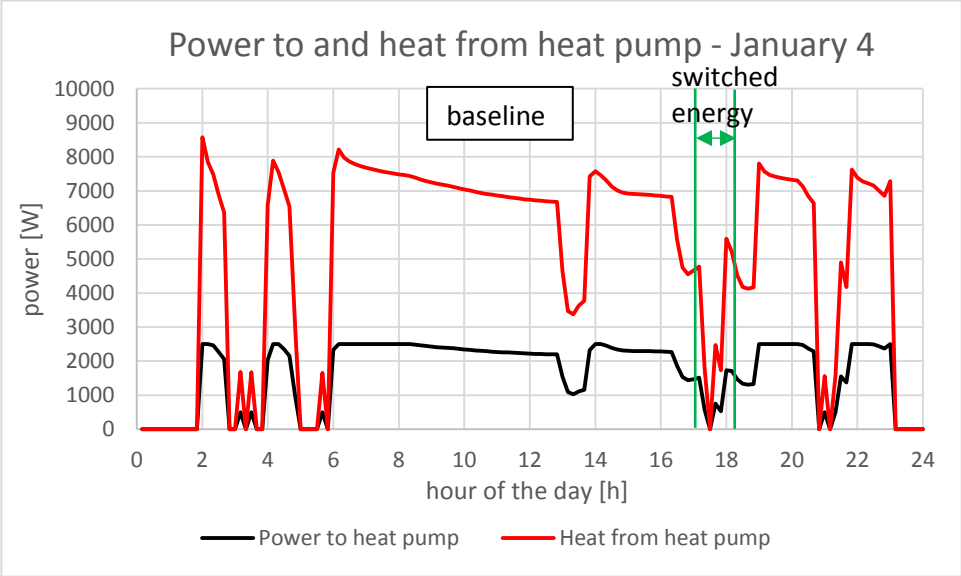

Figure 17. The power to the heat pump and the heat produced by the heat pump during January 4th for the baseline simulation.

The area between the green lines in figure 17 is when the set point temperature is decreased to 21°C in the 1U1H1D case (figure 18). The maximum power consumption by the heat pump is 2,500 kW. However, due to the free gains in the house (appliances (especially cooking appliances) and people) the heat pump would under traditional control run at reduced speed starting from shortly after 4pm, which leads to less shiftable power during the cooking peak starting at 5pm where the cooking delivers a large amount of energy to room 1. Thus, the amount of energy that may be shifted during the 1 hour and 20-minutes setback period in figure 16 is only 1.4 kWh with a mean power of just over 1 kW. 1.4 kWh is only 3.5 % of the total electricity demand of the heat pump during that day. When comparing figures 17 and 18, it is seen that there is only a small rebound effect for heating up the rooms after the small setback period. This is shown more clearly in figure 19, which shows the cumulated electricity to the heat pump for the two cases. Figure 19 shows that only a small amount of energy is shifted, which in the end leads to almost the same daily consumption for the two cases. 1U1H1D has only a 0.15 % higher electricity demand than for the baseline case.

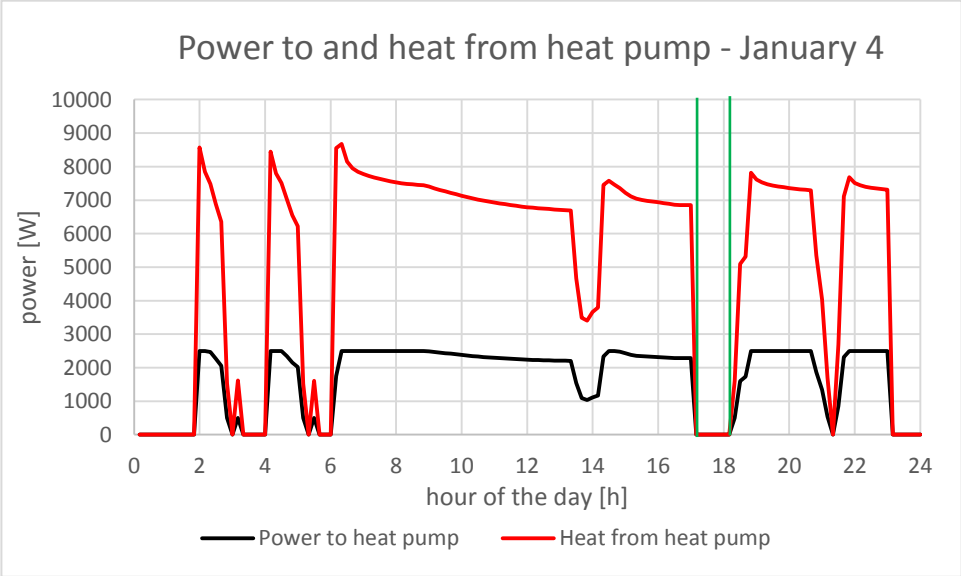

Figure 18. The power to the heat pump and the heat produced by the heat pump during January 4th for the 1U1H1D simulation.

4.3.1 December 21th

Figure 20 shows the room temperatures for December 21st from the 1U1H1D simulation. The day was rather cold with an ambient temperature between -14 and -5°C. The setback was carried out, but the controller immediately realizes that the setback is not possible, and it returns the operation to the normal set point. A more advanced controller would not have decrease the set point, as there was no energy flexibility available that day. However, due to the cooking peak, the room temperature of room 1 went above the set point, which resulted in the heating to this room being switched off. Therefore, it could be stated that the house delivered some energy flexibility to the grid by its normal control.

Figure 20 shows that the heat pump is too small for the very low ambient temperature during December 21st. However, this is the normal way of dimensioning heat pumps in Denmark in order not to "overinvest" in the heat pump. Normally, there would be a resistant heater in the heat pump for this rare occasion. Figure 20 shows that a heat pump needs to be oversized in order to be able to deliver energy flexibility during the entire heating season.

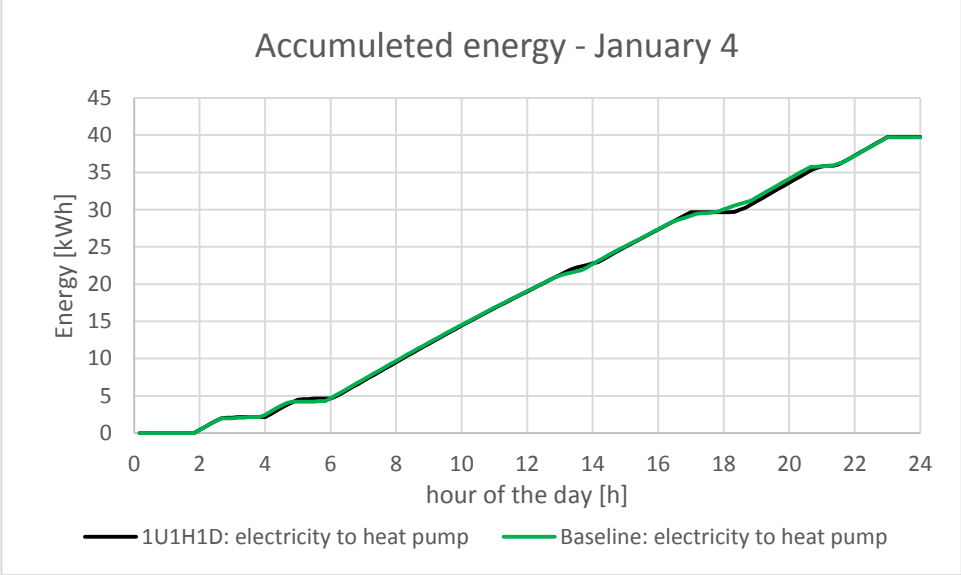

Figure 19. Comparison of the accumulated electricity to the heat pump for the two cases; 1U1H1D and the baseline simulation.

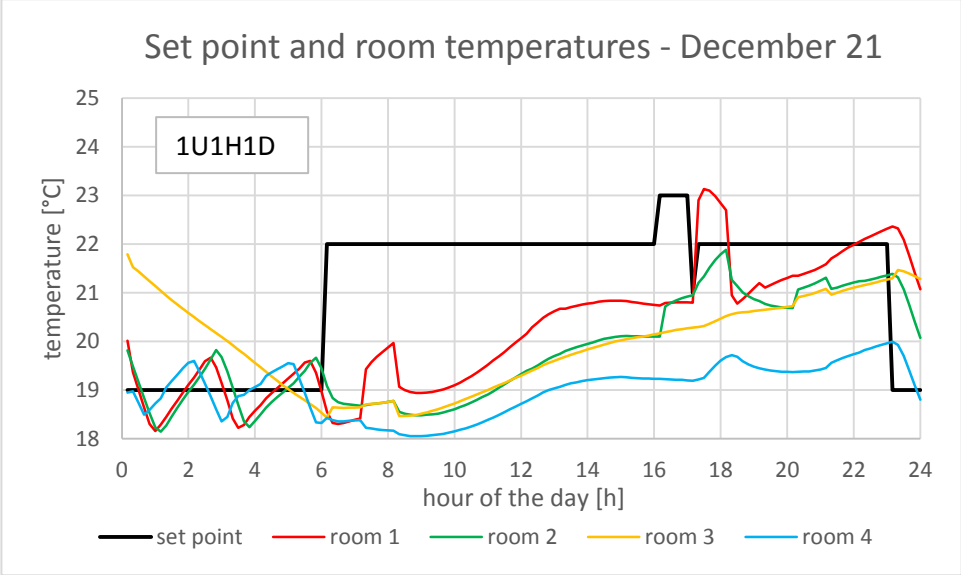

Figure 20. The evolution of the set point and the room temperatures during December 21st for the simulation 1U1H1D.

4.3.2 Shoulder season

Figure 16 and 20 shows situations where the heat pump had problems with the delivery of enough heat to the house. In the following, a situation during the spring is investigated: April 10th and April 11th, where the ambient temperature varied between 2 and 11°C. Much solar radiation is registered for April 10th, while only little solar radiation on April 11th. Figures 21 and 22 show the set point and the room temperatures during these two days.

The effect of solar radiation at a rather low angle is clearly seen in figure 21, especially for room 1. Room 1 overheats during April 10th, which results in the temperature of room 1 not reaching the setback set point before after the night setback was activated. The other rooms benefit as well from the solar radiation, but less than room 1. The setback set point is, therefore, returned to 22°C later during April 10th than during April 11th.

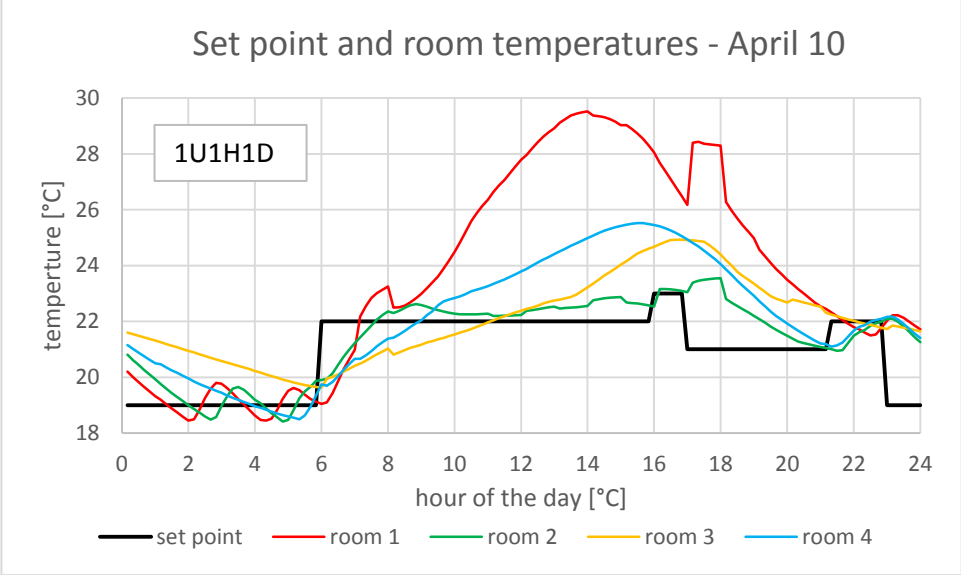

Figure 21. The evolution of the set point and the room temperatures during April 10th for the simulation 1U1H1D.

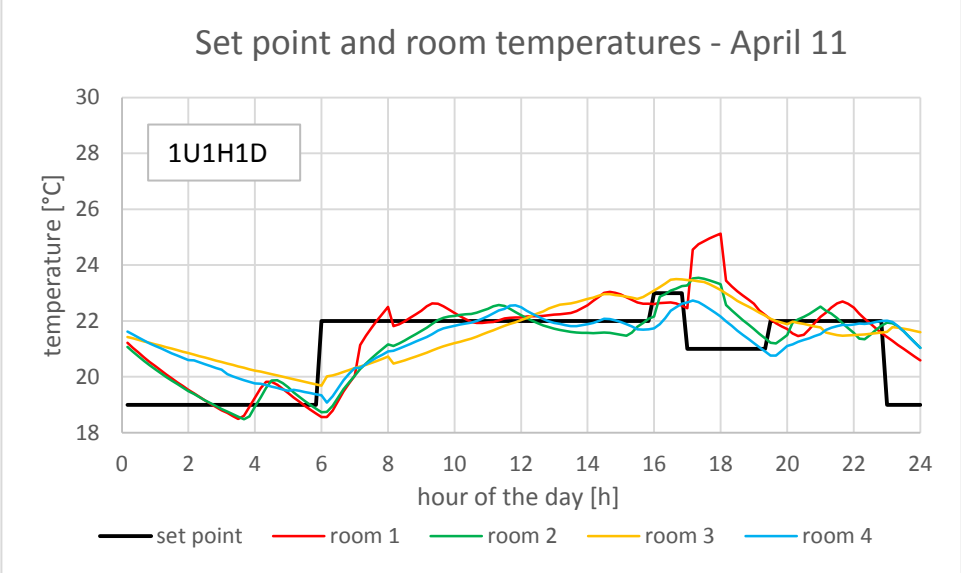

Figure 22. The evolution of the set point and the room temperatures during April 11th for the simulation 1U1H1D.

Table 1 compares the two days with regards to shifted energy.

Day	Duration of setback hours	Shifted energy[1] kWh	Mean shifted power[2] kW	Rebound[3] kWh
April 10	4.33	0.4	0.09	0.18
April 11	2.5	0.4	1.6	-0.40

Table 1. Comparison of April 10th and April 11th for simulation 1U1H1D.
[1] the amount of electricity to the heat pump that was used in the baseline case during the setback,
[2] the mean shifted power during the set back: shifted energy/duration of setback,
[3] difference between daily electricity demand during the baseline and 1U1H1D case.

Due to the solar radiation on April 10th, the duration of the setback is nearly twice as long as during April 11th. Figure 21 also shows that excess heating was only possible in room 2 as the

other room temperatures were above 23°C before the cooking peak. In spite of the solar radiation on April 10th, the shifted amount of energy is identical for the two days. The reason for this is shown in figures 23 and 24. During the baseline case the house needs heating much later on April 10th than on April 11th. What may surprise is that the setback during April 11th leads to a lower daily heat demand compared to the baseline, while for April 10th this leads to a slightly higher heat demand than the baseline. The reason for this is seen both in figures 21 and 22 as well as figures 23 and 24. In figures 21 and 22, it is seen that the room temperatures on April 10th are increasing just before the night setback, while the opposite is the case on April 11th. The reason for this is seen in figures 23 and 24, where the heating power just before the night setback (at 11pm) was more than twice as high on April 10th than on April 11th. Slightly changed conditions may have resulted in the opposite situation. This is, however, not investigated here, but it shows that the determination of the possible shiftable energy and the rebound effect are not easy tasks.

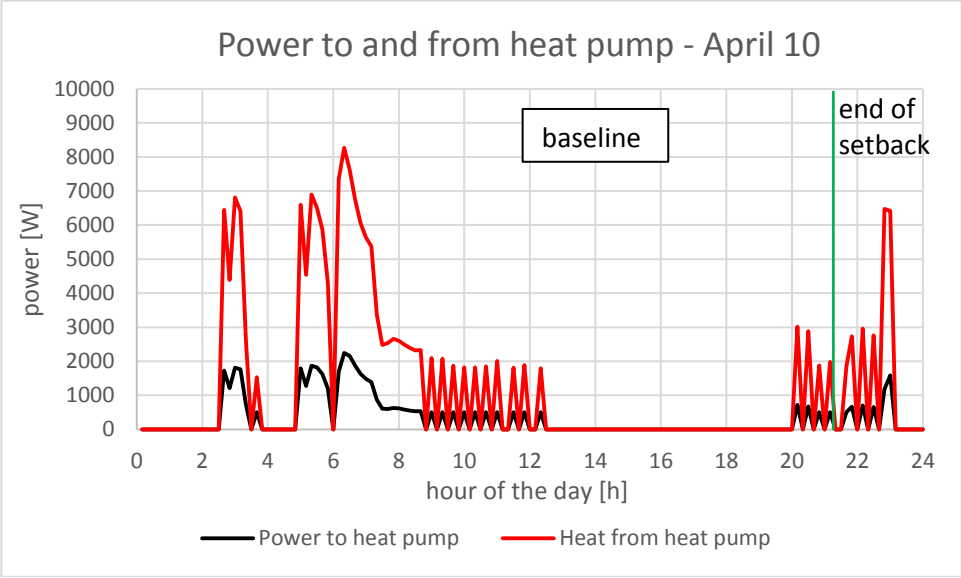

Figure 23. The power to the heat pump and the heat produced by the heat pump during April 10th for the baseline simulation.

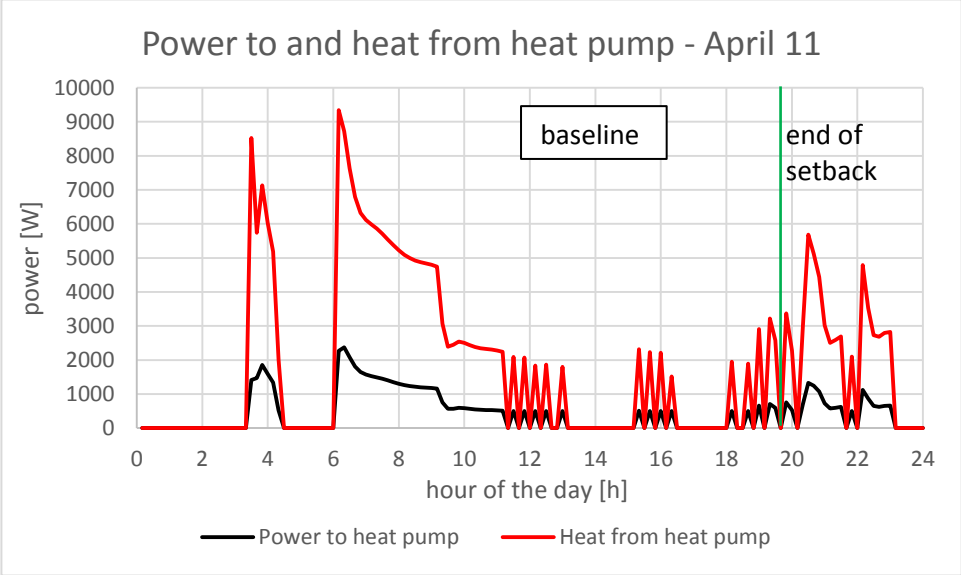

Figure 24. The power to the heat pump and the heat produced by the heat pump during April 11th for the baseline simulation.

Table 1 gives a mean shiftable power of 0.09 kW during the setback on April 10th. However, the shiftable amount of energy is first available by the end of the setback period, which means that the operator of the power grid will not have any energy flexibility from this house during the cooking peak, but first at 8pm. This illustrates that single numbers like shiftable energy (here in the form of electricity) and mean power during a setback period may contain too little information for the system operators, e.g. DSO (Distribution System Operator) or BRP (Balance Responsible Parties) to be able to make decisions on how to utilize available energy flexibility.

Although the amount of shiftable energy/electricity, the shiftable mean power, and the duration of setback for a single house may not be valuable information for controlling the energy networks. These values may be of interest at an aggregated level when controlling many heat pumps. Therefore, the values will be investigated on an annual basis in the following, as they also contain important information about the single house. The values will be referred to as performance indicators in the following.

4.3.3 Performance indicators for 1U1H1D

The former sections showed that the performance indicators are not fixed values, - they change over the year. This is investigated in the following.

Figure 25 shows the duration of the setback using the 1U1H1D control strategy. The figure shows that the mean duration of the setback during the main heating season is around one hour with the 1U1H1D control strategy. The values in figure 25 are rather scattered, so in order to be able to compare with other control strategies, figure 25 has been transformed to figure 26, which shows the mean monthly setback durations.

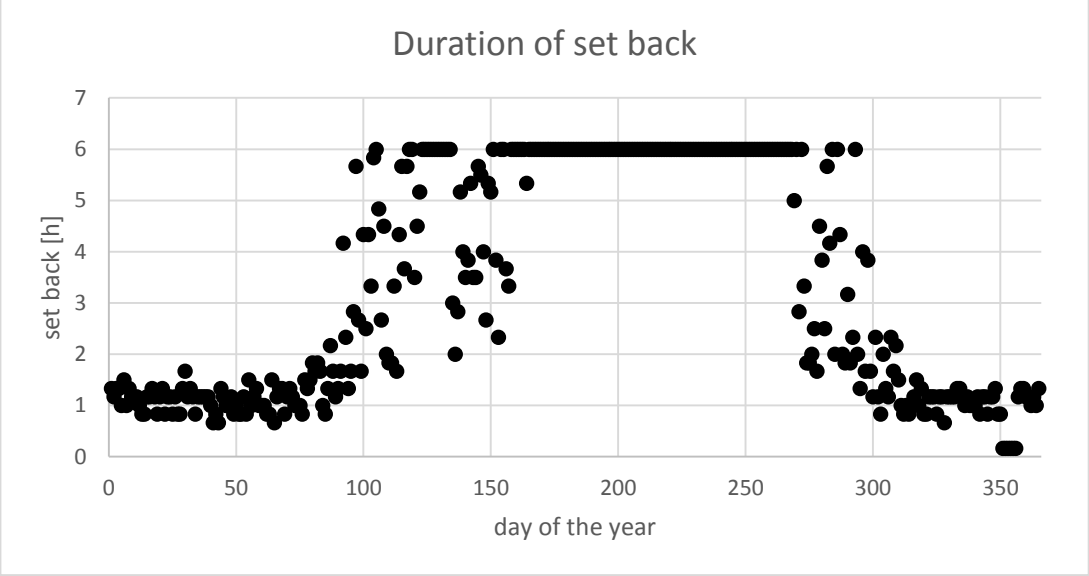

Figure 25. Daily duration of the setback using the 1U1H1D control strategy.

Figure 27 compares the maximum daily amount of shiftable electricity (from figure 14) with the actual obtainable shiftable electricity using 1U1H1D as control strategy. Figure 27 shows that typically less than 10 % of the maximum amount of shiftable electricity can actually be utilized in this case.

Figure 28 shows the obtainable amount of shiftable mean power as a function of the mean daily ambient temperature. As for figure 15, there is a clear correlation between the mean daily ambient temperature and the shiftable mean power although the values in figure 28 are more scattered than in figure 15. Figure 29 shows the obtainable daily amount of shiftable energy as a function of the mean daily ambient temperature.

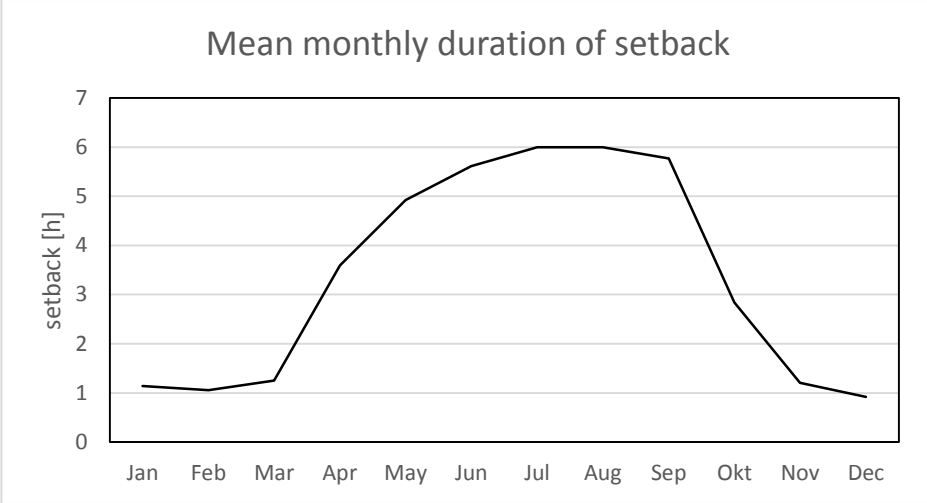

Figure 26. Mean monthly duration of the setback using the 1U1H1D control strategy.

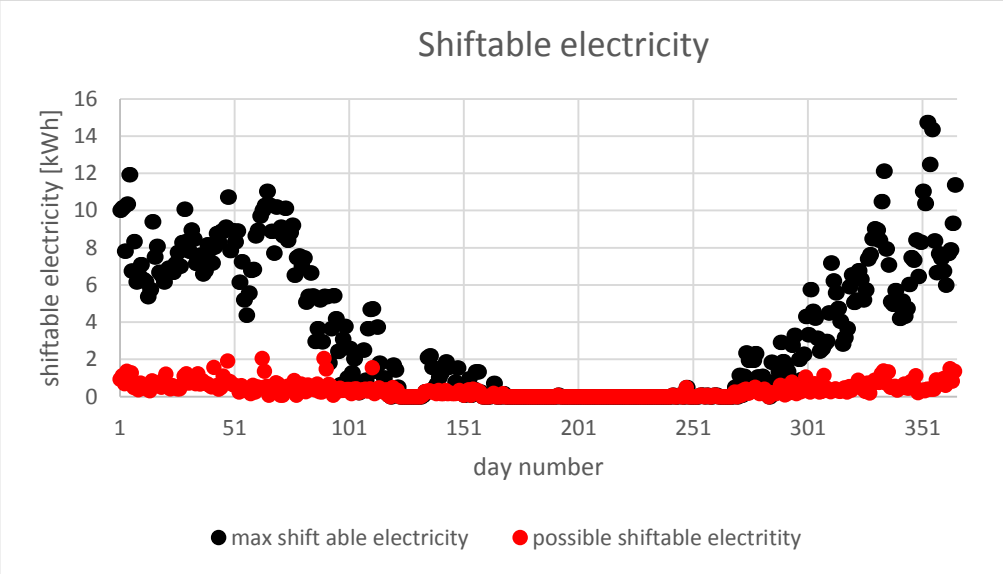

Figure 27. Obtainable amount of shiftable daily electricity compared with the maximum amount of shiftable electricity using the 1U1H1D control strategy.

Figures 26-29 show rather short setback periods, little obtainable daily amount of shiftable energy and little shiftable mean power when using the 1U1H1D control strategy for the actual house. In the following section, others of the control strategies mentioned in section 4.2 will also be investigated.

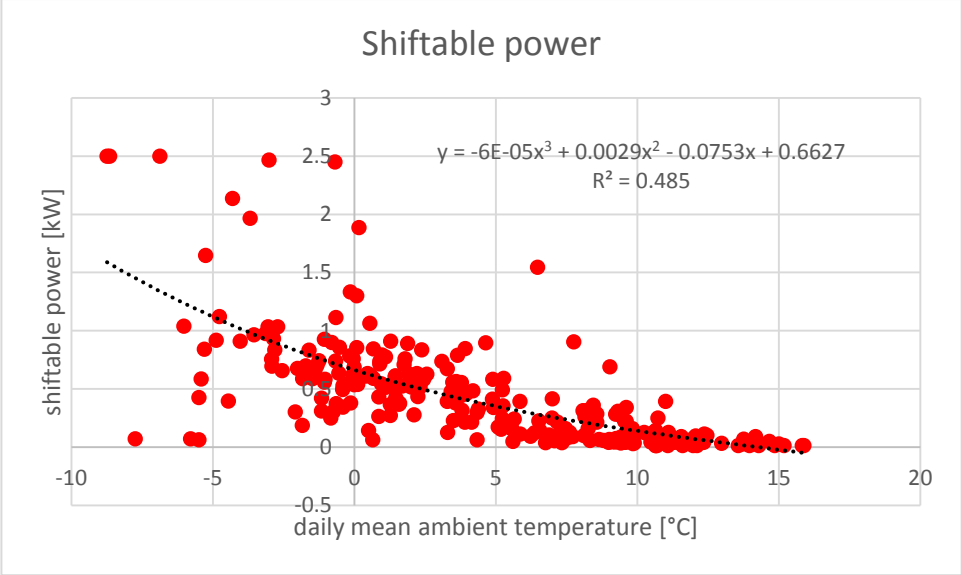

Figure 28. Obtainable amount of shiftable mean power dependent on the mean daily ambient temperature using the 1U1H1D control strategy.

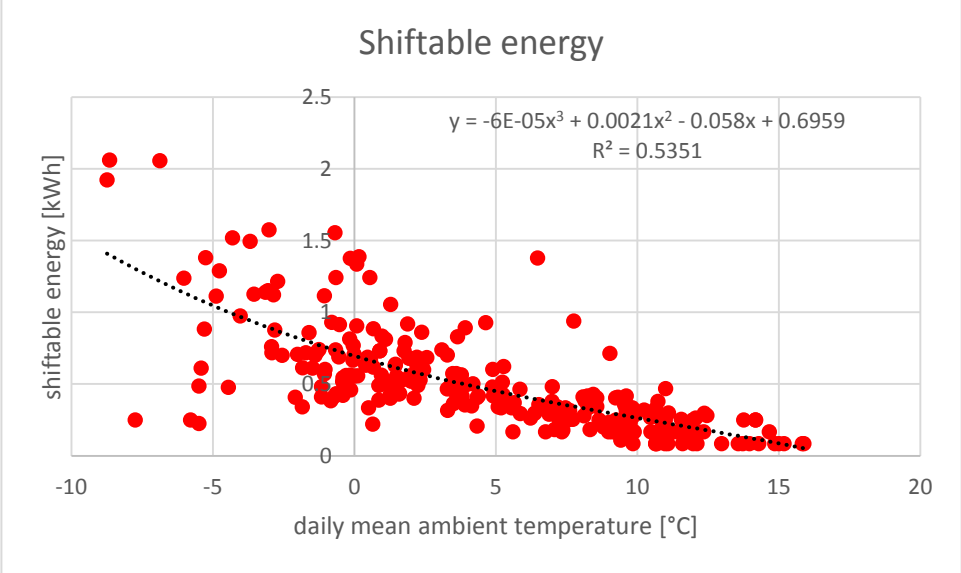

Figure 29. Obtainable amount of shiftable daily energy dependent on the mean daily ambient temperature using the 1U1H1D control strategy.

4.4 Results from all parameter variations

Due to the specific design and the use of the 1970's house, only the following simulations turned out to be necessary:

0U0H1D: T_l = 21°C, no excess heating
0U0H2D: T_l = 20°C, no excess heating
1U1H1D: T_l = 21°C, T_h = 23°C starting at 4pm
1U2H1D: T_l = 21°C, T_h = 23°C starting at 3pm
2U1H1D: T_l = 21°C, T_h = 24°C starting at 4pm

The results from these simulations will be evaluated in the following.

4.4.1 Only setback of the set point

Two cases where only the set points were set back were simulated: 1 and 2 K decease at 5pm denoted 0U0H1D and 0U0H2D.

Figure 30 shows the result for April 11th for the two cases.

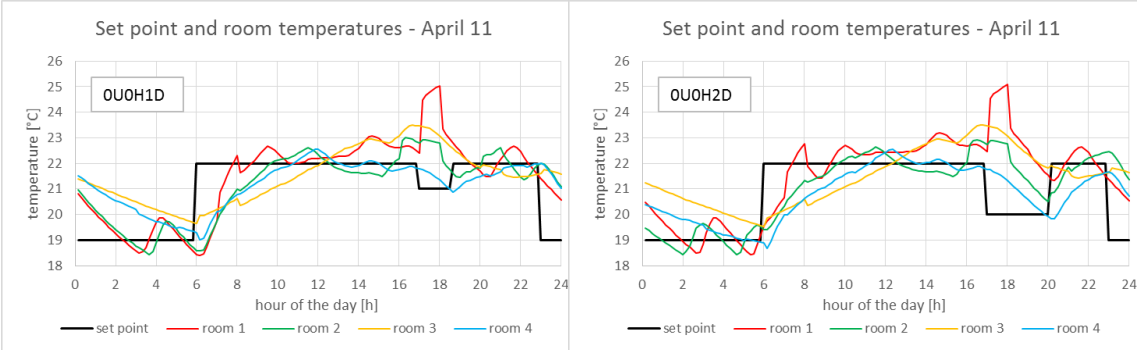

Figure 30. Comparison of possible duration of the setback period with a set point decrease of 1 K (left) and 2 K (right) on April 11th.

Figure 30 shows that in this case for April 11th, the duration of the setback is almost twice as long with a decrease of the set point with 2 K (3 hours and 10 minutes) compared to a decrease of 1 K (1 hour and 40 minutes). The duration of the setback for April 10th is already long with a 1 K decrease of the set point: 4 hours and 20 minutes (see figure 21). In this case changing to a setback of 2 K will only increase the duration of the setback to 5 hours and 50 minutes or to 10 minutes before the night setback. Thus, the increase of the duration of the setback is 19 % in this case.

Due to a very fast decrease in the temperature of room 2 and 4, the increase of the duration of the setback, when going from a decrease in set point from 1 K to 2 K, is only 10 minutes during January 4th.

As a setback of the set points during December 21th is not possible due to a too small heat pump – see figure 20, lowering the setback set points will not change this.

Figure 31 shows the mean monthly possible duration of the setback for the two cases. The figure shows that during the main heating season, the setback can be increased by an average of around half an hour when going from the 0U0H1D to 0U0H2D control.

Figure 32 shows the possible daily amount of shiftable energy and the mean shiftable power for the two investigated cases. The possible amount of daily shiftable energy increases due to the increase in the possible duration of the setback. As an example, at a mean daily ambient temperature at -5°C, the possible amount of shiftable energy is 1.1 kWh with a 1 K setback and 1.6 kWh with a 2 K setback. However, the mean shiftable power is very similar due to the fact that these values are defined by dividing the amount of daily mean energy with the duration of the setback.

However, as described in the former section it is not known when the shiftable energy and power are available during the setback period, and with an increasing duration of the setback, this uncertainty increases as well.

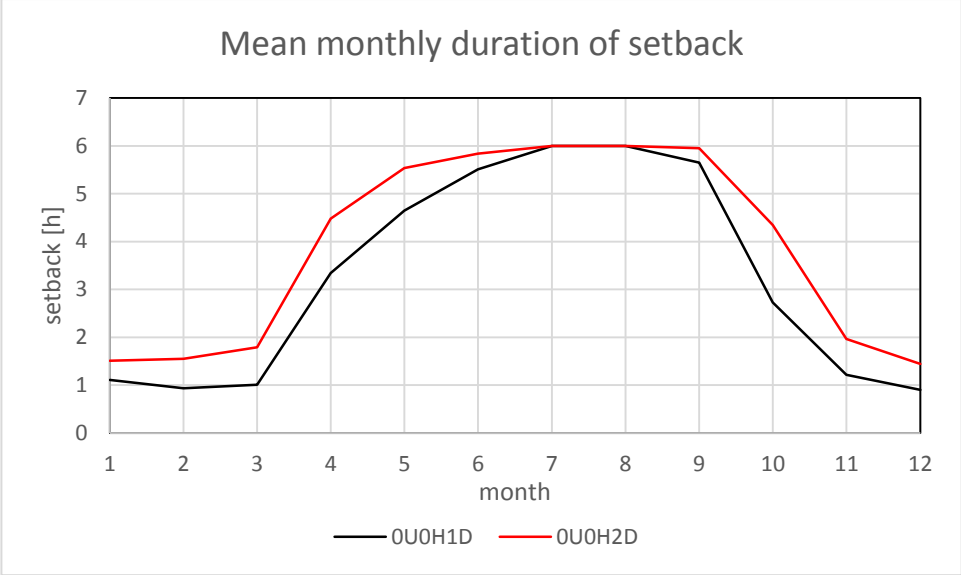

Figure 31. Comparison of possible mean monthly duration of the setback period with a set point decrease of 1 K (0U0H1D) and 2 K (0U0H2D).

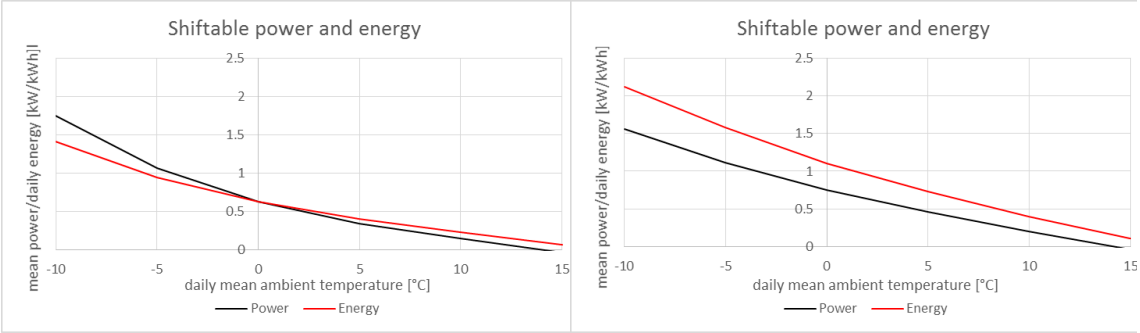

Figure 32. Comparison of (trend lines for) the possible amount of daily shiftable energy and the mean shiftable power at a set point decrease of 1 K (0U0H1D - left) and 2 K (0U0H2D - right).

4.4.2 Excess heating of the house before the setback

Three simulations have been carried out, all with a setback of 1 K. The three simulations are:

- 1U1H1D: 1 K increase in set point 1 hour before the cooking peak
- 2U1H1D: 2 K increase in set point 1 hour before the cooking peak
- 1U2H1D: 1 K increase in set point 2 hour before the cooking peak

The excess heating hardly increased the energy flexibility compared to only setback (described in the former section) for these cases as seen in figures 33 and 34. The reason for this is shown in figures 16 and figures 20-22 as well as in the following figures 35 and 36.

Figure 35 shows that only room 2 is influenced by the excess heating. However due to the fast decrease of the temperature in this room, the mean monthly duration of the setback is hardly increased because of the excess heating. Figures 16 and 35 show that all rooms during January 4th receive heat two hours before the cooking peak (except for room 2 which stops being heated around one hour before the cooking peak). The figures also show that, the temperatures do not exceed 23°C during the hour before the cooking peak. Thus, for January 4th there is no difference between 1U1H1D, 2U1H1D and 1U2H1D.

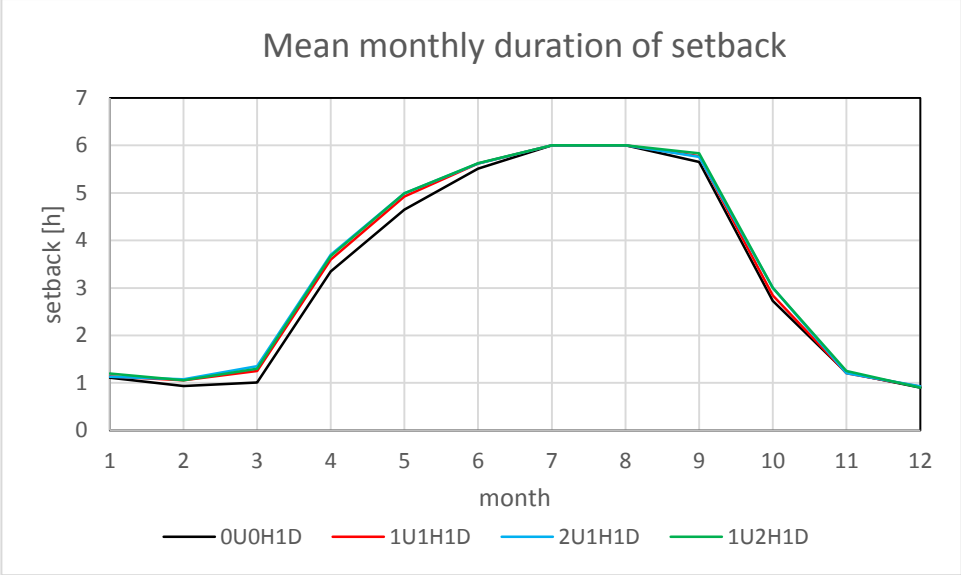

Figure 33. Comparison of possible mean monthly duration of the setback period with only setback (0U0H1D) and with excess heating (1U1H1D, 2U1H1D and 1U2H1D).

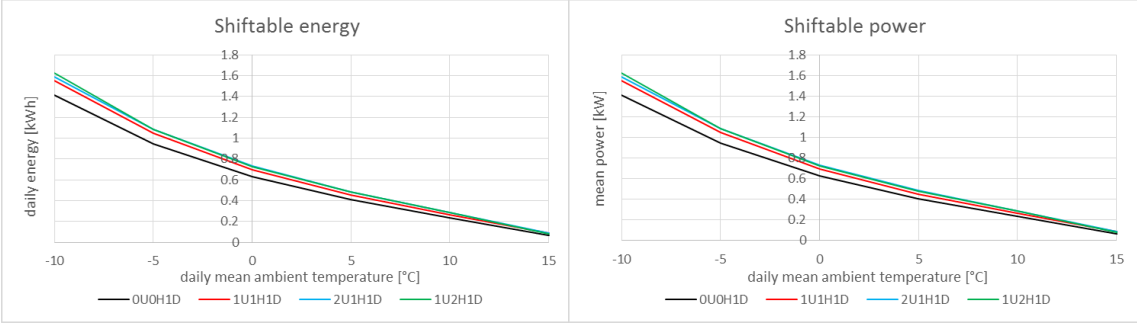

Figure 34. Comparison of (trend lines for) the possible amount of daily shiftable energy (left) and the mean shiftable power (right) with only setback (0U0H1D) and with excess heating (1U1H1D, 2U1H1D and 1U2H1D).

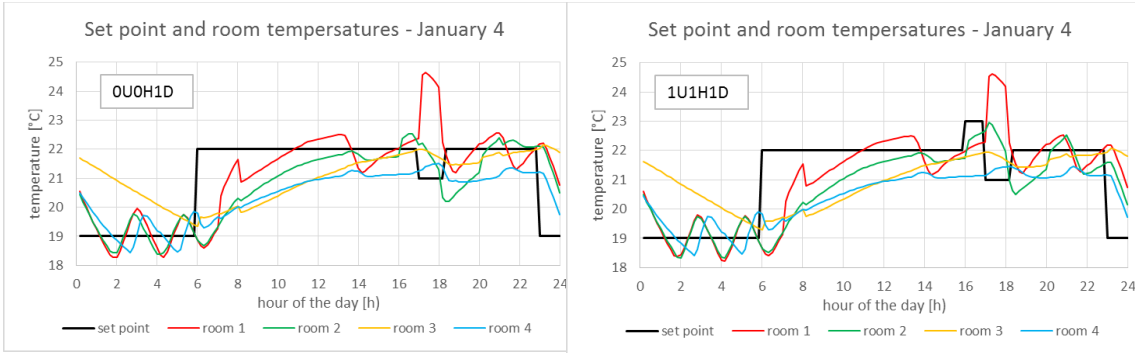

Figure 35. Comparison of the possible duration of the setback period with only a set point decrease of 1 K (left) and 1 K excess heating during one hour before the setback (right) on January 4th.

As explained in the former section no energy flexibility is available for December 21th as the heat pump is too small to reach the set point of 22°C – see figure 20. Thus, excess heating is of course not possible for this day.

Figure 36 shows the possible duration of the setback with only a decrease of the set point temperature and with excess heating for April 10th.

The possible duration of setback of the four situations in figure 36 is:

0U0H1D: 1 hour and 40 minutes
1U1H1D: 2 hours and 30 minutes
2U1H1D: 2 hours and 30 minutes
1U2H1D: 2 hours and 50 minutes

Prior to the cooking peak, only room 4 calls for heat. However, as this is the room that ends the setback on this day, the duration of the setback is increased with 50 % for a one-hour duration of the excess heating. In this case excess heating with a set point of 23 and 24°C is identical as it is room 4, which ends the setback, and it is not influenced by a higher excess heating set point. An excess heating of two hours extend the duration of the setback with 20 minutes as the temperature of room 4 is higher at the beginning of the cooking peak. A two-hour excess heat at a set point of 24°C would not lead to a longer duration of the setback as all room temperatures are below this set point.

Due to the high room temperatures during April 10th – see figure 21, the duration of the setback is identical for only setback and one and two-hour excess heating at 23°C: 4 hours and 20 minutes, while the one-hour excess heating at 24°C adds 30 minutes to the duration of the setback.

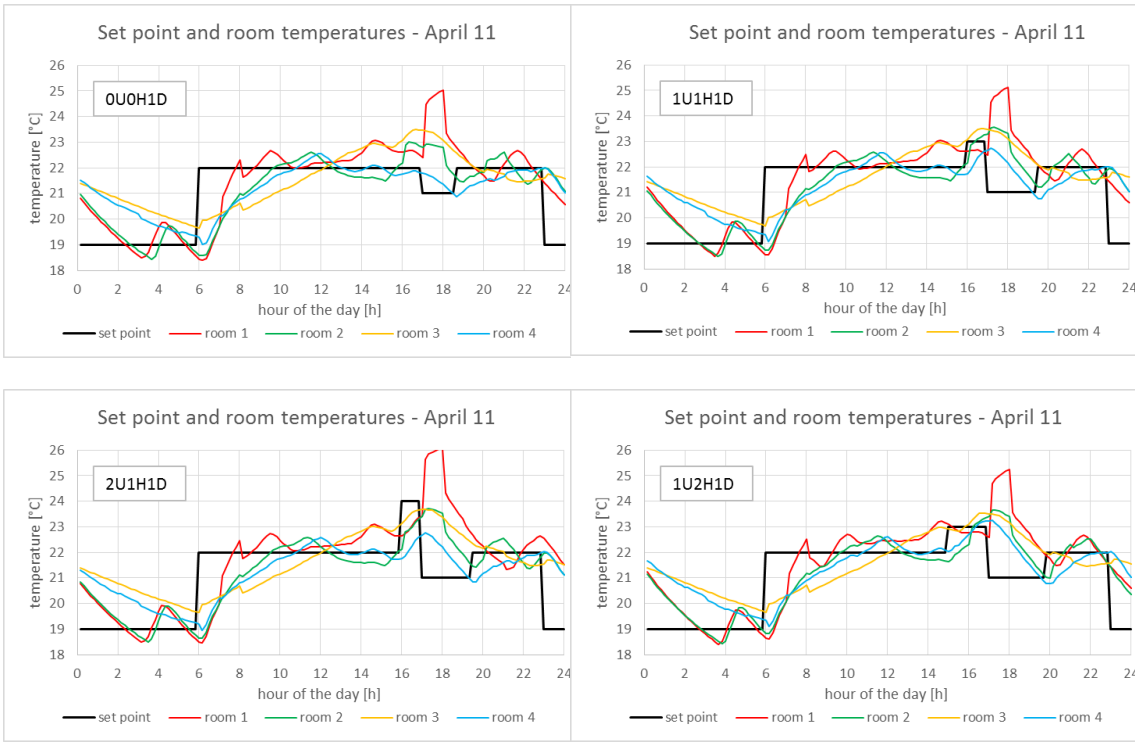

Figure 36. Comparison of possible duration of the setback period with only a set point decrease of 1 K (top left) and with excess heating for April 11th (1U1H1D, 2U1H1D and 1U2H1D).

4.4.3 Annual electricity demand of the heat pump

Table 2 shows the annual electricity demands for the six simulated cases.

For this specific house, there is no real difference in the energy demand of the heat pump. One main reason is that most of the electricity used for appliances during the cooking peak is delivered to the room with the highest energy demand. Only setback leads to a bit lower electricity demand due to slightly lower room temperatures during the cooking peak and only a

slight rebound effect. 1U1H1D has the same electricity demand as the baseline case, while the two cases with more excess heating have a slightly higher electricity demand.

Simulation	Annual electricity demand kWh	Difference compared to baseline %
Baseline	4,877	-
0U0H1D	4,860	-0.3
0U0H2D	4,845	-0.7
1U1H1D	4,876	-0.02
2U1H1D	4,880	+0.06
1U2H1D	4,884	+0.14

Table 2. Comparison of the necessary annual electricity demand of the heat pump for the six simulation cases.

In other investigations, a higher electricity demand when utilizing energy flexibility to minimize the annual costs of electricity has been reported. As an example, (Parvizi, 2016) reports a 30 % saving on the energy bill, however, with an 8 % larger energy demand. This simulation was carried out with a 48-hour prediction horizon using perfect forecasts.

4.4 Conclusion

Although the investigated control of the heat pump is very simple and the design as well as the use of the house are not ideal for obtaining energy flexibility, the exercise revealed several interesting aspects.

The controllable energy flexibility is very dependent on any free gains from solar radiation and appliances, which occur close to or during a period when energy flexibility is needed from a house. In the present investigated cases, the heat input of 3.2 kW to the main room during the one-hour cooking peak reduced the possible controllable/obtainable energy flexibility during this period. If the morning peak had been investigated, instead this would lead to more obtainable energy flexibility due to less free gains, Moreover, if the persons of the house closely after breakfast leave for job, school, etc., it would be possible to further decrease the set point temperature of the rooms. Figures 17, 23 and 24 show that there is a high heat demand in the morning, while less in the afternoon/early evening. Figure 23 shows that the switchable energy on April 10th does not occur until after 8pm and not during the cooking peak.

Furthermore, the simulations show that in order to be able to offer energy flexibility to the grid during the entire heating season, the heat pump needs to be oversized. However, the additional costs of an oversized heat pumps need to be compared with the possible income from being able to offer the extra energy flexibility, which a larger heat pump makes possible.

Based on the findings from the above simulations with a very simple control strategy for obtaining energy flexibility it can be stated that in order to gain maximum energy flexibility there is a need for a more advanced controller - and preferably a controller, which includes weather forecast and forecast of free gains in the house. Instead of having an identical increase and decrease of the set point in all rooms a more advanced controller could differentiate according to the actual conditions. For instance in figure 22, it is room 4, which causes the stop of the setback. Room 2 would otherwise have stopped the setback half an hour later, while room 1 and 3 seems to have been able to go without heat for a couple of more hours. A more advanced controller could, e.g. based on PIR sensors, determine if it was necessary to start heating room 2 and 4 or the heat pump could shortly have been switched on at low speed in order to stabilize the temperature of these two rooms around the setback set point instead of increasing the room temperature of all rooms to 22°C.

It seems that the night setback is responsible for the very little rebound effect as the room temperatures often would not have reached the normal set point of 22°C after a setback before the night setback switches off the heat pump.

In this document the possible energy flexibility of the house is described in terms of:

- the monthly mean duration of the possible setback – e.g. figure 26
- the shiftable daily amount of energy/electricity as a function of the daily mean ambient temperature – e.g. figure 32
- the mean shiftable power as a function of the daily mean ambient temperature – e.g. figure 32

These parameters are as shown in the above sections very dependent on the actual conditions at the time of the day for activating of the setback. Thus, they cannot be utilized for an exact determination of the possible energy flexibility from the house at a certain moment. Furthermore, the three values will vary over the year. However, for an aggregator, who looks for houses to include in his/her portfolio, the values may be useful when scanning for suitable houses in a specific area.

5. Test in the OPSYS test rig

The parametric analysis in chapter 4 was performed with a fast simulation program as the test rig runs at real-time. Both the simulation on the test rig computer and the annual fast simulation program use the same house model. However, while the heat pump in the annual simulation is a very simple model (see section 2.1) as it does not i.a. consider the thermal capacity of the heat pump, the test rig includes a real heat pump with all the physical complexity this leads to. Furthermore, the flow rates in the four rooms are determined by the simulation in the annual simulations while the simulation program at the test rig only controlled the opening and closing of the valves (telestats). The actual flow rates are determined by the hydronic of the test rig.

This chapter investigates how well the annual simulations can create similar energy flexibility as the test rig.

In the following, results from the OPSYS test rig are compared to similar results obtained from the annual simulation program. Two cases have been tested in the test rig: eight days in January and seven days in April in order to compare with the results already presented in chapter 4.

5.1 January

Figure 37 shows the obtained room temperatures in the test rig simulation of the house for the period January 2nd-9th and figure 38 shows the ambient temperature during the same period. The effect of solar radiation to room 1 is clearly seen in figure 37. However, it is rather difficult to see the duration of the setback in figure 37. Therefore, figure 39 shows only the resulting set point for the room temperatures. Due to the low ambient temperature the duration of the setback is rather short as also shown in figure 16 (January 4th) and figure 20 (December 21th).

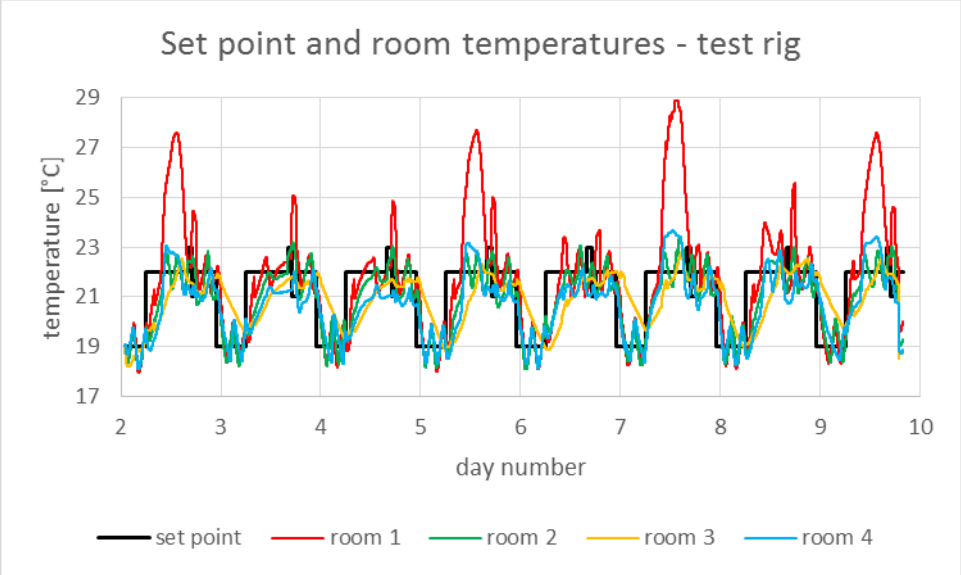

Figure 37. Room temperatures obtained from the OPSYS test rig for the period January 2nd-9th.

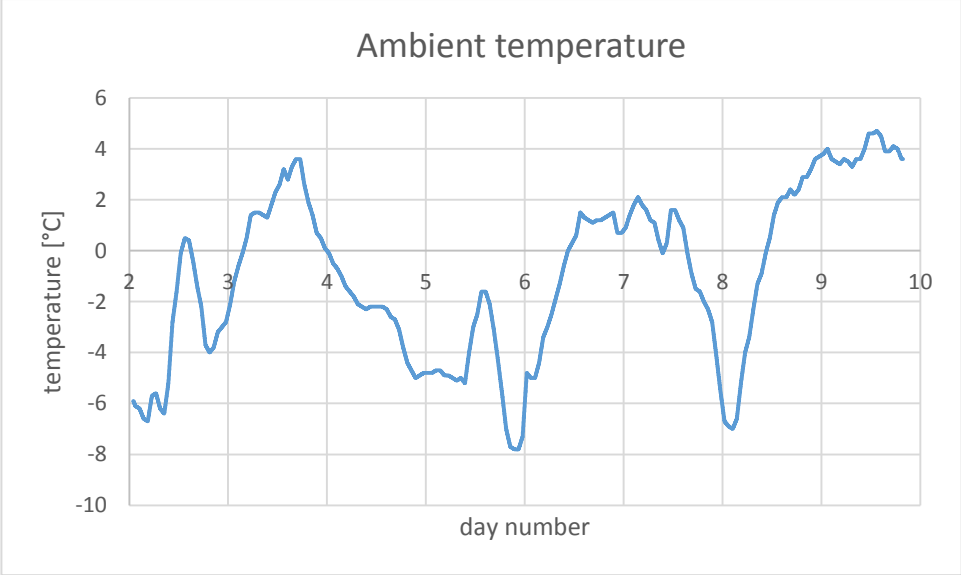

Figure 38. Ambient temperatures for the same period as figure 37.

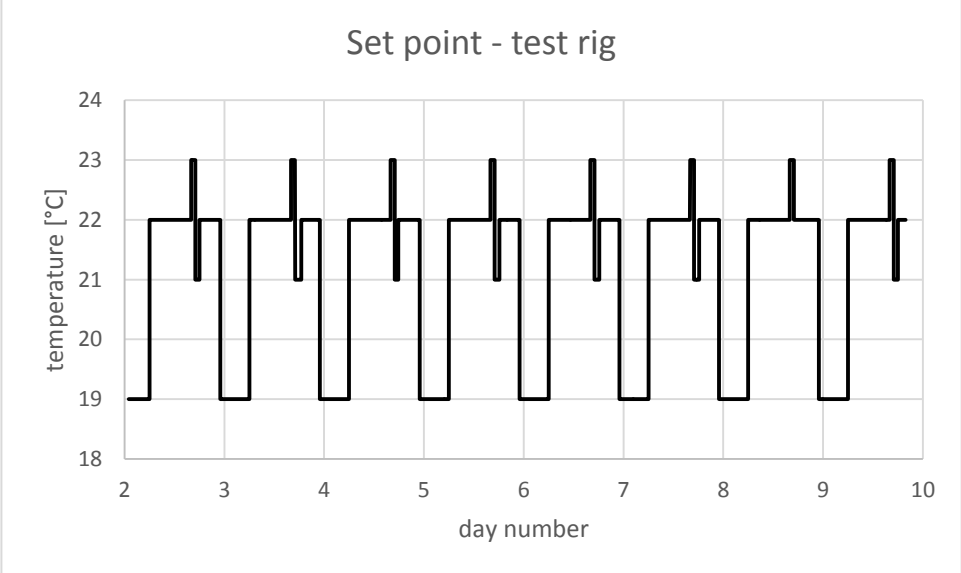

Figure 39. The set point of the room temperatures from figure 37.

Figures 40 and 41 show the room temperatures and the set point for January 4th: figure 40 shows the results from the test rig and figure 41 the results from the annual simulation. The development of the temperature profiles is much alike between the two simulations. The development of the set point is more squared in figure 40 than in figure 41. This is due to the time step of the simulation. On the test rig (figure 40), the time step was 15 seconds while the time step of the annual simulation was 10 minutes.

The slight difference between the room temperatures in the two figures is as explained above that the test rig includes a real heat pump with all its complexity and the flow rates were not completely identical.

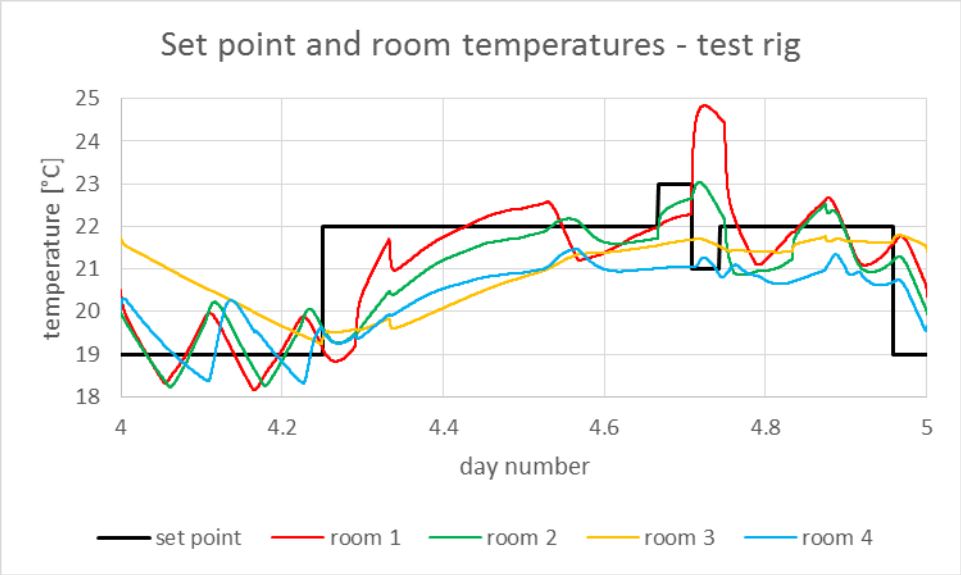

Figure 40. January 4th from figure 37.

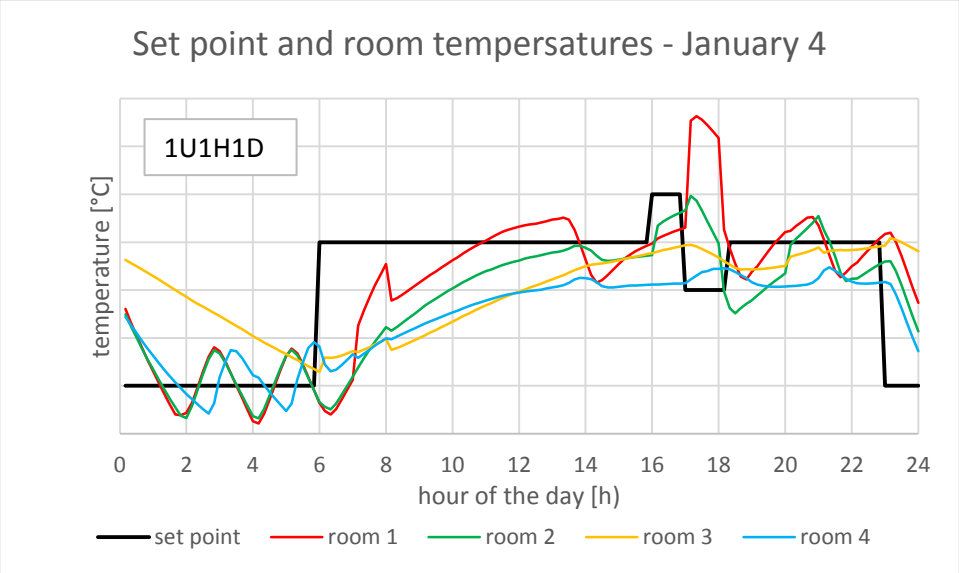

Figure 41. January 4th from the annual simulation – identical to figure 16.

Similar to figure 20 figure 39 shows that during the winter there is often no energy flexibility available – e.g. January 8th.

5.2 April

Figures 42-44 are identical to figures 37-39 except that the period here is April 10th-16th.

Figures 42 and 44 show as expected a longer duration of the setback due to higher ambient temperatures and more solar radiation. For day 104 (April 14th), the duration of the setback lasts almost until the night setback. For the following day, the duration of the setback lasts beyond the time of the night setback. The difference between these two days is approximately a 2 K higher ambient temperature on day 105.

Figures 45-48 compare the room temperatures obtained by the test rig with the room temperatures obtained by the annual simulation.

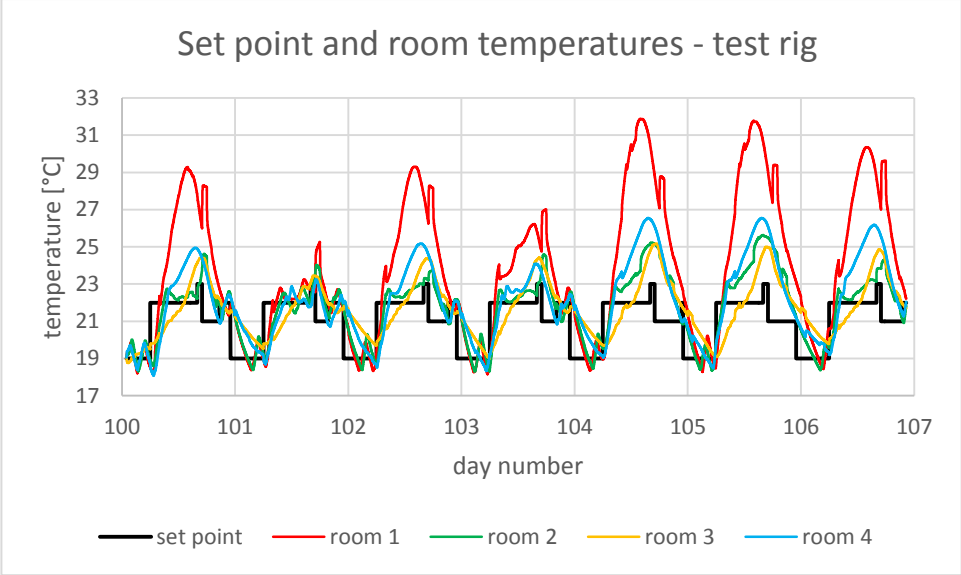

Figure 42. Room temperatures obtained from the OPSYS test rig for the period April 10th-16th.

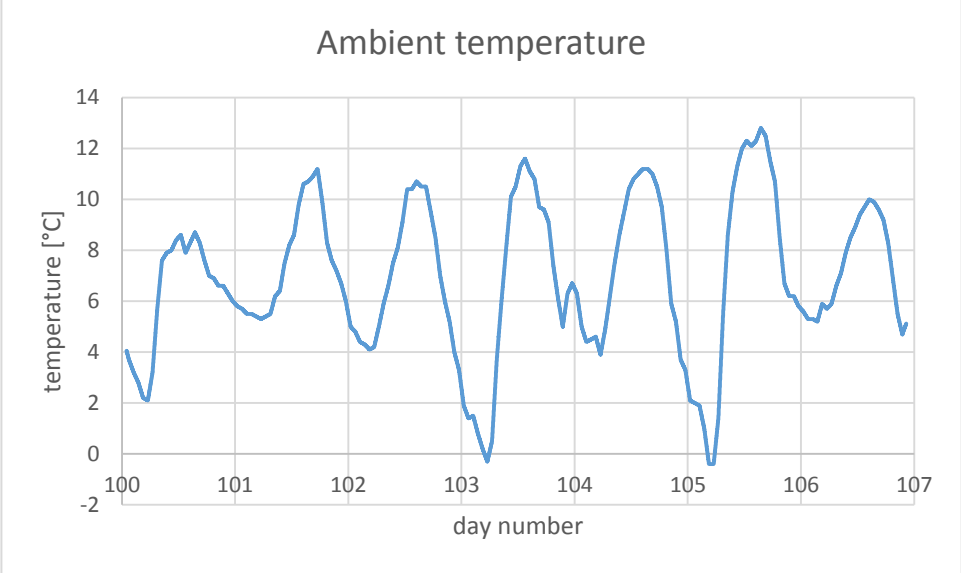

Figure 43. Ambient temperatures for the same period as figure 42.

The good agreement between the test rig and the annual simulation is again seen, - best for April 11th (figures 47 and 48). For April 10th the room temperatures of room 3 and 4 are somewhat lower at the test rig during the cooking peak than seen from the annual simulation, while for room 2 this temperature is a bit higher. The duration of the setback is a bit shorter in the test rig than in the annual simulation for April 10th, while the duration of the setback is similar for the two cases on April 11th.

The measured and the simulated power consumption of the heat pump is shown in figures 51 and 52 for April 10th-11th. The test was started on day 100. This explains the measured power consumption from the start of the test, whereas this consumption is not present in the graphs with the simulated results. However, the start-up consumption is small in the test rig as there is much less water in the test rig than in the heat emitting system of a real house.

The less good agreement between the room air temperatures from the test rig and the annual simulation for April 10th is, therefore, due to the fact that the test in the test rig was started on

April 10th. This is seen in figures 49 and 50 which show April 12th, where the test had run for two days. April 12th (day 102) is as seen in figure 42 similar to April 10th (day 100). Figures 49 and 50 show almost identical patterns for the room air temperatures and a similar duration of the setback.

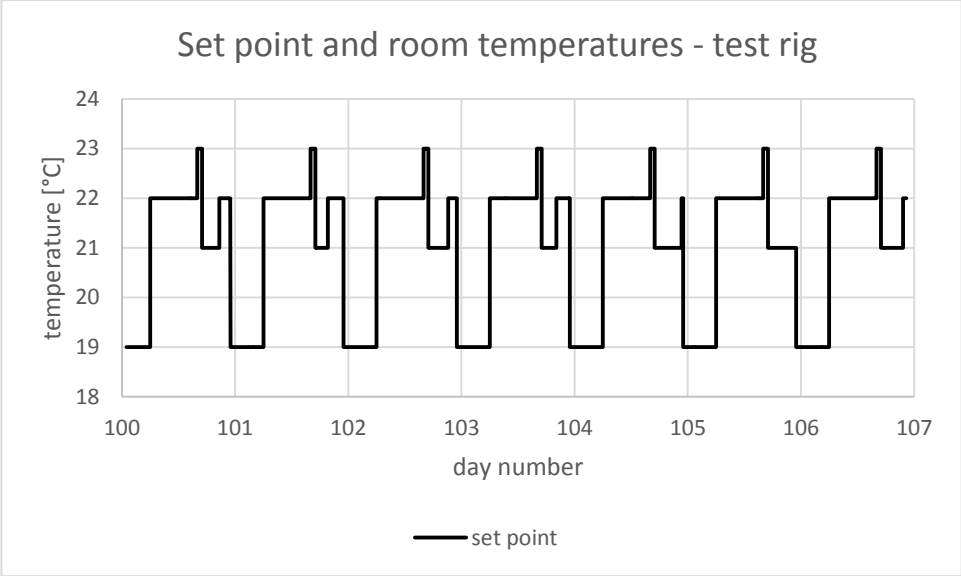

Figure 44. The set point of the room temperatures from figure 42.

Based on the above, it seems that the test rig only needs a one day start-up period before the temperatures of the test rig and the simulated performance of the house have reached stable conditions, and the obtained room air temperatures from the test rig and the annual simulations become comparable. This is important as tests in the test rig run real-time, so more than one day for obtaining stable conditions would seriously prolong a test.

The patterns of the electricity consumption are different in the measured and the simulated cases (figures 51-54), but the consumption occurs at more or less the same time. The reason for the difference in consumption patterns is as explained earlier, that the heat pump in the annual simulation is represented by a very simple equation. The efficiency of the heat pump in the annual simulation is expressed as a dependency of the heat demand and the ΔT between the temperature of the brine to the heat pump and the needed forward temperature to the heat emitting system. There is no thermal capacity of the heat pump. Furthermore, the simulated heat pump is assumed to be continuously regulated in the area of 500-2500 W while it is on/off controlled below 500 W. The latter is clearly seen in figure 52 in the morning of day 100. The physical heat pump is differently on/off controlled as seen in figure 51 in the morning of day 100. Here, the heat pump is allowed to deliver more heat at each on-period leading to fewer starts and stops during on/off control.

To determine whether the above is also correct when the test rig has been in operation for several days, figures 53 and 54 show the measured and simulated power consumption of the heat pump for day number 104-106 (April 14th-15th). Figures 53 and 54 do not change the above conclusion, but they show that the continuous control of the heat pump is also different in the two cases as the maximum measured power to the heat pump is 1,836 W while in the simulated case it is 2,420 W.

Figures 40 and 41 as well as figures 47-50 show that the simple model of the heat pump in the annual simulation gives a good representation of the room air temperatures. The reason for this is that the inertia (thermal capacity) of the house, which acts as a low pass filter between the heat input to the underfloor heating system and the pattern of the room air temperatures. Even fast steps in the set point of the room air temperatures are handled well. However, fig-

ures 51-54 show that the annual simulation program could benefit from a more detailed model of the heat pump when considering the performance of the heat pump. This was attempted, but the heat pump module of Dymola (in which the house model was created) was too slow to be used in the annual simulations. This was why a simple model of the heat pump was chosen.

Work has been done in the OPSYS project to speed up the Dymola model of heat pumps. This model could be utilized for shorter simulation periods where the dynamics of the neat pump and the telestats is of special interest.

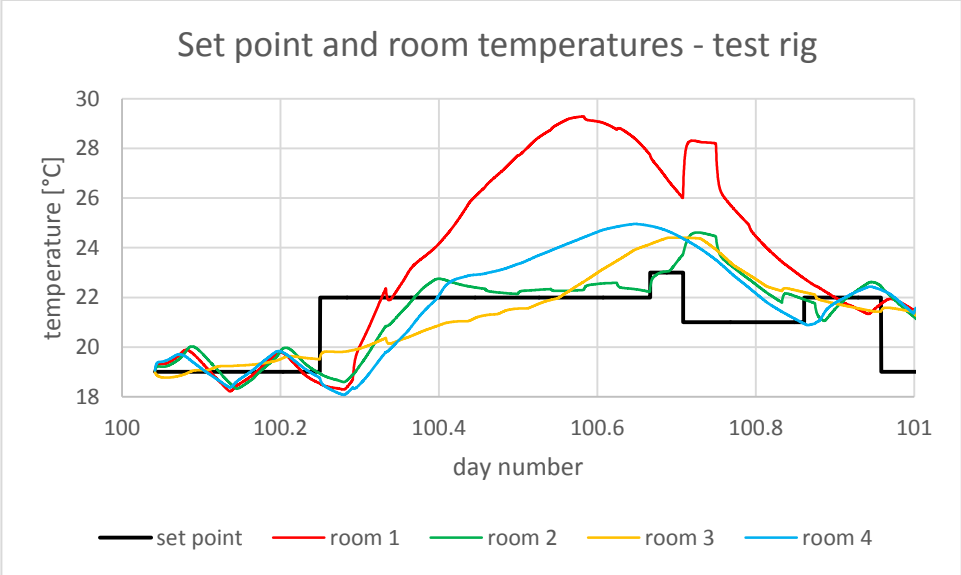

Figure 45. April 10th – day 100 from figure 42.

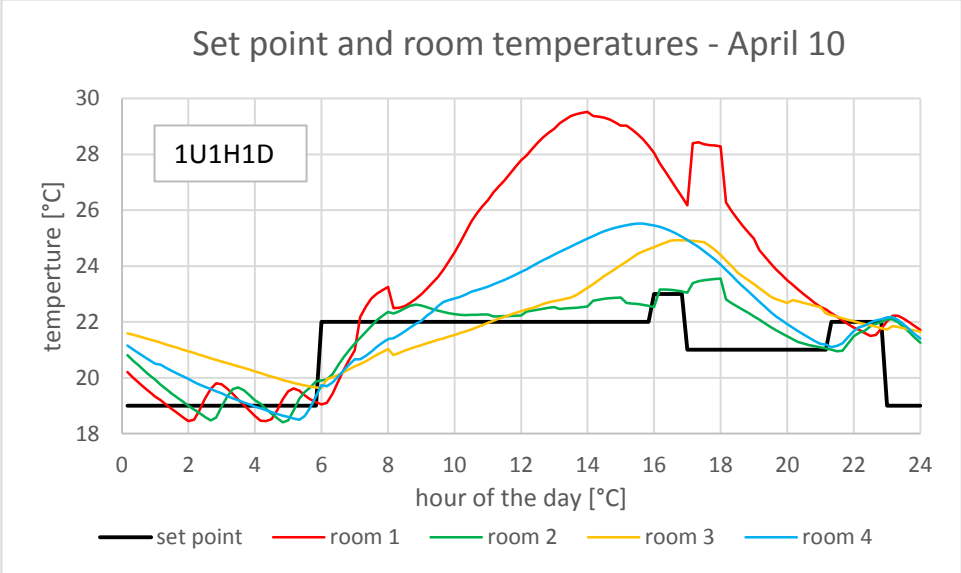

Figure 46. April 10th from the annual simulation – identical to figure 21.

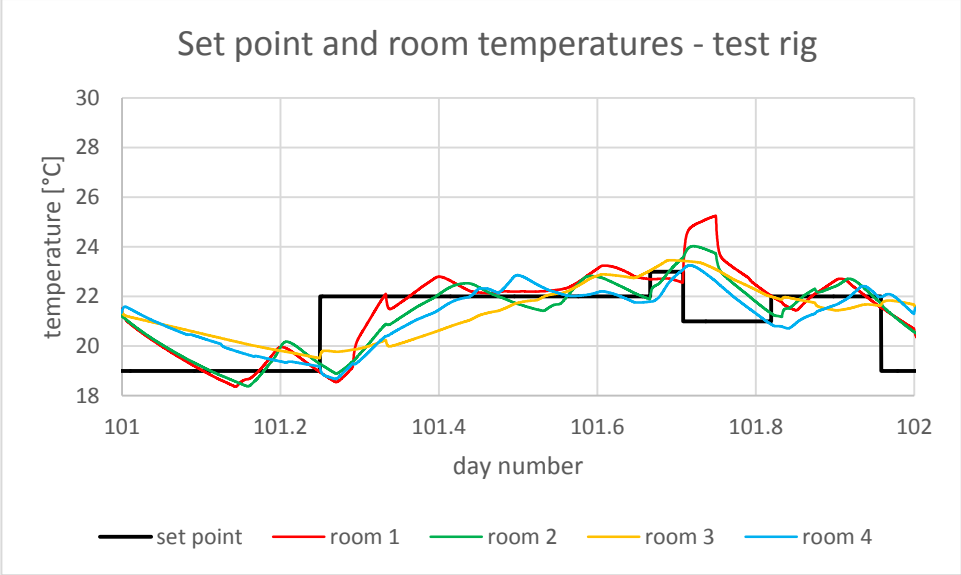

Figure 47. April 11th – day number from figure 42.

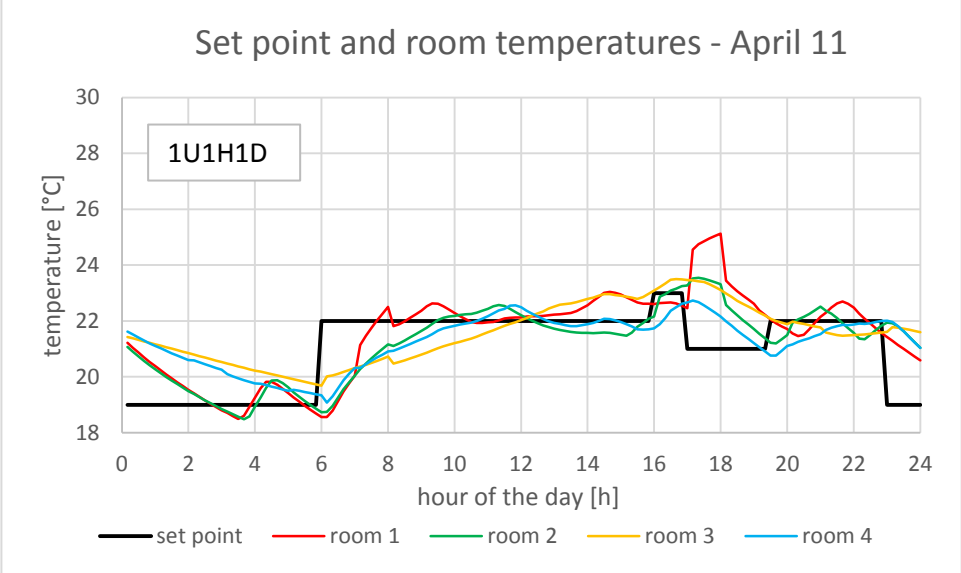

Figure 48. April 11th from the annual simulation – identical to figure 22.

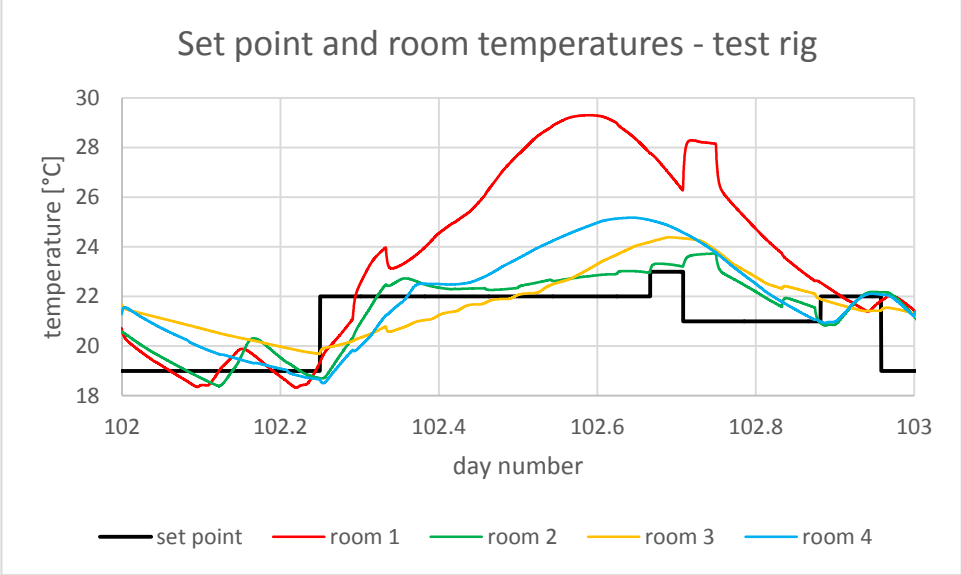

Figure 49. April 12th – day 102 from figure 42.

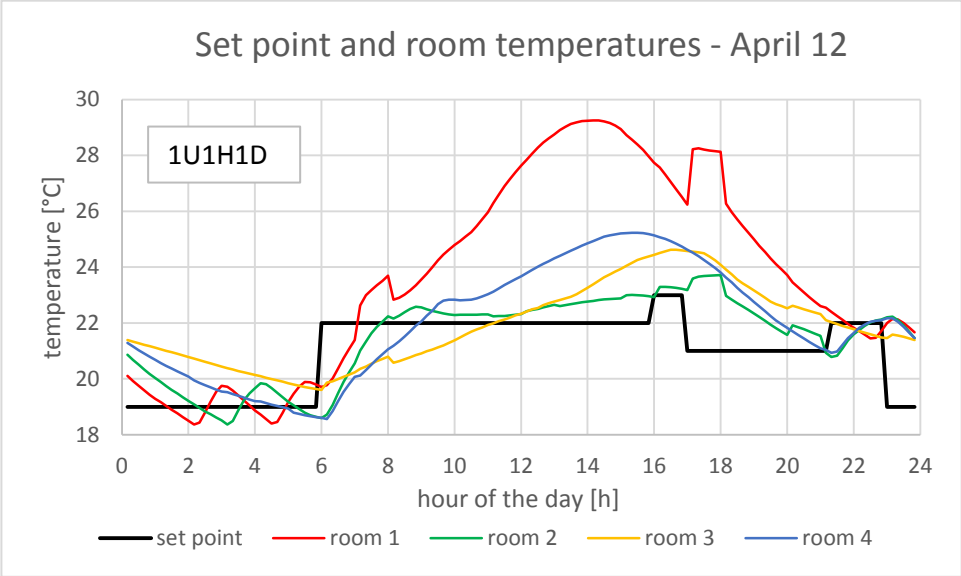

Figure 50. April 12th from the annual simulation.

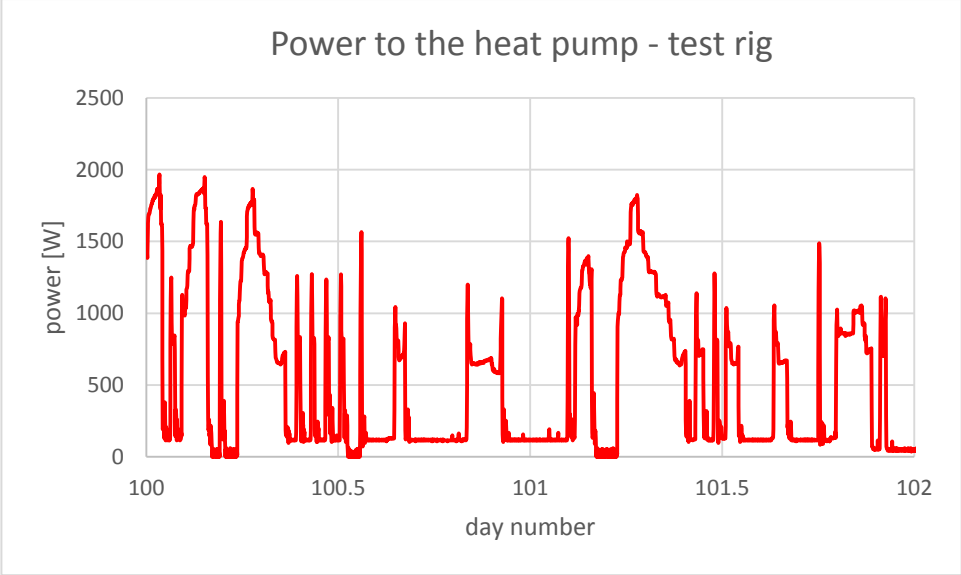

Figure 51. Power to the heat pump in the test rig – April 10th-11th.

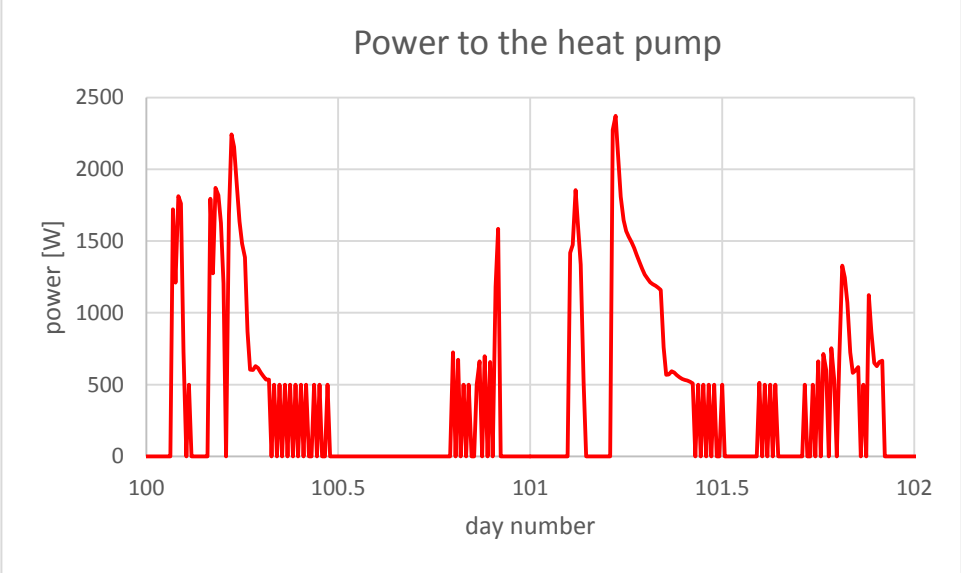

Figure 52. Power to the heat pump in the annual simulation – April 10th-11th.

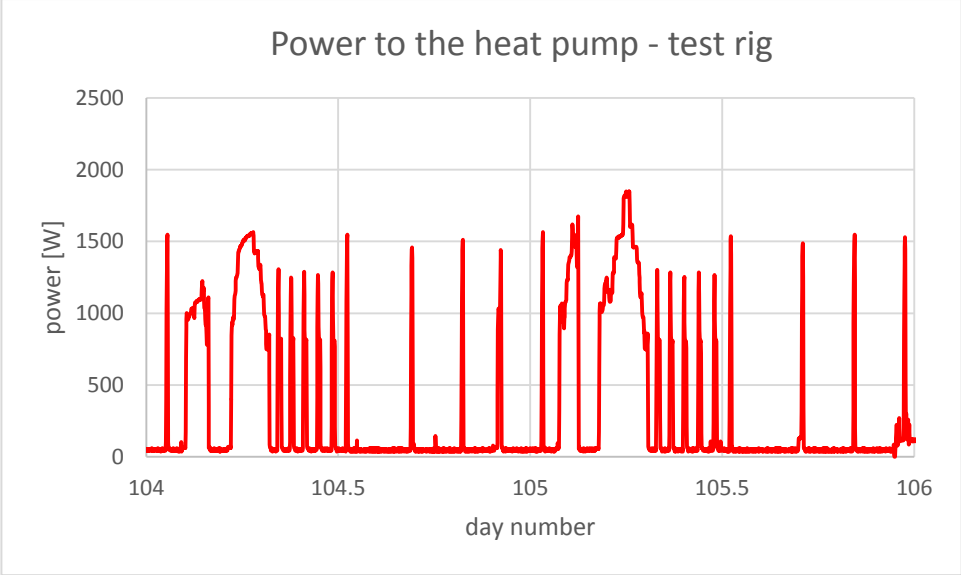

Figure 53. Power to the heat pump in the test rig – April 14th-15th.

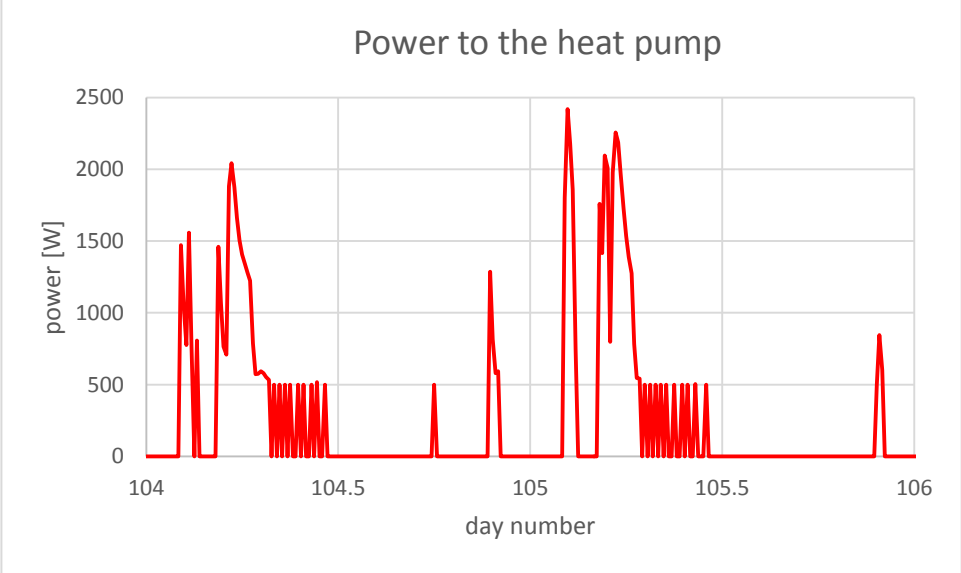

Figure 54. Power to the heat pump in the annual simulation – April 14th-15th.

5.3 Conclusion

Despite the simple representation of the heat pump in the annual simulation program and dissimilar flow rates in the four circuits of the underfloor heating system, there is good agreement between the obtained measured and simulated energy flexibility expressed in terms of the duration of switching-off the heat pump. The patterns of the room air temperatures from the test rig and the annual simulation are also similar

It is, therefore, believed that the OPSYS test rig also will be capable of testing more advanced controls including different set points for the room temperatures as well as partly opening of the telestats (valves of the four circuits in the floor heating system). The latter in order to control the flow rate to each circuit in order to optimize the heat delivered to each room.

6. Conclusion

The tests with a very simple controller for obtaining energy flexibility of a house with a heat pump have shown that the two tools give not only comparable but also realistic results. The tools are, therefor, assessed to be useful when developing also more advanced controllers for obtaining energy flexibility.

The controllable energy flexibility is very dependent on any free gains from solar radiation and appliances, which occur close to or during a period when energy flexibility is needed from a house. In the present investigated cases, the heat input of 3.2 kW to the main room during the one-hour cooking peak reduced the possible controllable/obtainable energy flexibility during this period. If the morning peak had been investigated, instead this would lead to more obtainable energy flexibility due to less free gains, Moreover, if the persons of the house closely after breakfast leave for job, school, etc., it would be possible to further decrease the set point temperature of the rooms.

Furthermore, the simulations show that in order to be able to offer energy flexibility to the grid during the entire heating season, the heat pump needs to be oversized. However, the additional costs of an oversized heat pumps need to be compared with the possible income from being able to offer the extra energy flexibility, which a larger heat pump makes possible.

Based on the findings from the above simulations with a very simple control strategy for obtaining energy flexibility it can be stated that in order to gain maximum energy flexibility there is a need for a more advanced controller - and preferably a controller, which includes weather forecast and forecast of free gains in the house. To optimize the energy demand of a house according to the needs of the grids, there is a need for a Rule Base Controller, a Model Predictive Controller (MPC), an Economic Model Predictive Controller or a well-trained controller based on Neural Network. Although neural network based controllers and MPCs have been studied in the OPSYS project (Jensen et al, 2018) with the purpose of optimizing the performance of a heat pump in connection with a heat emitting system without considering the grid, the funding of the project has not allowed for an investigation of these types of advanced controllers with the achievement of energy flexibility in mind.

References

Hedegaard. K. et al, 2012. Wind power integration using individual heat pumps – Analysis of different heat storage options. Energy 47 pp 284-293, 2012. Elsevier. http://vbn.aau.dk/da/publications/wind-power-integration-using-individual-heat-pumps--analysis-of-different-heat-storage-options(e34692df-b080-4c75-a5ad-bdb1f2a4b26e).html.

Jensen. S.Ø., Olesen, M.F. and Paulsen, O., 2014. Lightweight underfloor heating sys-tem and the impact on the efficiency of heat pumps (partly in Danish, however, not the part containing fluctuation of the flow rate). Danish Technological Insti-tute, February 2014. ISBN: 978-87-93250-01-7. At https://www.teknologisk.dk/strategisk-forskningscenter-for-energineutralt-byggeri/varmepumper-og-gulvvarmeanlaeg/38997,3

Jensen, S.Ø., Christensen, C.H., Jørgensen, D.M. and Huet, J., 2016. Smart Meter Case Study. Danish Technological Institute. Report part of the iPower Project. At https://www.teknologisk.dk/ipower/39033

Jensen, S.Ø., Marszal-Pomianowska, A.J., Lolline, R., Pasut, W., Knotzer, A., Engelmann, P., Stafford, A. and Reunders, G., 2017. IEA EBC Annex 67 Energy Flexible Buildings EBC special issue of Energy and Buildings, October 2017. http://www.sciencedirect.com/science/article/pii/S037877881731702

Jensen, S.Ø. et al, 2018. Combines optimization of heat pumps and heat emitting systems. Danish Technological University, Aalborg University and Modelon. May 2018. At www.teknologisk.dk/39663

Klein, K., Killinger, S., Fischer, D., Streuling, C., Salom, J. and Cubi, E., 2016. Comparison of the Future Residual Load in Fifteen Countries and Requirements to Grid-Supportive Building Operation. EuroSun 2016. http://www.uibcongres.org/eurosun/ponencia.en.html?mes=120&ordpon=1

Poulsen, S., Jensen, S.Ø, Larsen, E.O. and Borup, R., 2017. The good installation of heat pumps (in Danish). Danish Technological Institute and Insero. 2nd edition. January 2017. At www.teknologisk.dk/39663

Parvizi, J., 2016. Modelling and Control for Price Responsive Electricity Loads. Department of Applied Mathematics and Computer Science, Technical University of Denmark. http://orbit.dtu.dk/en/publications/modeling-and-control-for-price-responsive-electricity-loads(7ff027e9-cb51-4baa-b28f-d940a9e94a1e).html.